ERDC/CRREL TR-20-11

US Army Corps of Engineers®
Engineer Research and Development Center

ERDC
ENGINEER RESEARCH & DEVELOPMENT CENTER

Evaluation of Solid-Polymer-Modified Asphalt Mixtures

Phase 1: Construction and Performance Testing of Field Pavement Sections

Christopher J. DeCarlo, Mohamed H. Elshaer, Allan Wheeler, and Jared I. Oren

September 2020

Cold Regions Research and Engineering Laboratory

The U.S. Army Engineer Research and Development Center (ERDC) solves the nation's toughest engineering and environmental challenges. ERDC develops innovative solutions in civil and military engineering, geospatial sciences, water resources, and environmental sciences for the Army, the Department of Defense, civilian agencies, and our nation's public good. Find out more at www.erdc.usace.army.mil.

To search for other technical reports published by ERDC, visit the ERDC online library at https://erdclibrary.on.worldcat.org/discovery.

ERDC/CRREL TR-20-11
September 2020

Evaluation of Solid-Polymer-Modified Asphalt Mixtures

Phase 1: Construction and Performance Testing of Field Pavement Sections

Christopher J. DeCarlo, Mohamed H. Elshaer, Allan Wheeler, and Jared I. Oren

U.S. Army Engineer Research and Development Center (ERDC)
Cold Regions Research and Engineering Laboratory (CRREL)
72 Lyme Road
Hanover, NH 03755-1290

Final Report

Prepared for Headquarters, U.S. Army Corps of Engineers
Washington, DC 20314-1000

Under PE 62784 / Project T26 “Innovative Construction Materials for Cold Regions”

Abstract

The durability of flexible pavements in cold regions is a challenge due to the impact of environmental conditions and seasonal variations. Other studies have investigated several modifiers as potential solutions to address cold climate durability of asphalt mixtures. Among these modifiers, polymer modification has shown promise.

This study investigated the addition of solid polymer to asphalt mixtures to improve the performance and structural capacity of the material. Four test sections were constructed with different solid-polymer dosage rates: unmodified control, 2.5% polymer, 5% polymer, and 7.5% polymer by weight of binder. Falling weight deflectometer (FWD) testing was conducted at each test section to evaluate the structural capacity and to identify the performance benefits of the solid-polymer-modified mixtures. This study conducted a comprehensive analysis, including maximum pavement deflection, deflection bowl parameters, backcalculation analysis, structural number, and impulse stiffness modulus.

The field investigation results revealed structural benefits in test sections with the solid-polymer-modified mixture (7%–30% increase in stiffness, depending on the dosage rate). Results suggest that solid-polymer modification could be useful in improving the stiffness of asphalt pavements without compromising durability. Therefore, further investigations should evaluate the durability of the solid-polymer-modified asphalt pavements under different environmental conditions.

Contents

Figures and Tables

Figures

Tables

Preface

This study was conducted for the U.S. Army Corps of Engineers under PE 62784 / Project T26, "Innovative Construction Materials for Cold Regions." The technical monitor was Mr. Jared Oren, U.S. Army Engineer Research and Development Center, Cold Regions Research and Engineering Laboratory (ERDC-CRREL).

The work was performed by the Engineering Resources Branch of the Research and Engineering Division, ERDC-CRREL. At the time of publication, Mr. Jared Oren was Branch Chief; Mr. J. D. Horne was Division Chief; and Mr. Nicholas Boone, ERDC Geotechnical and Structures Laboratory (GSL), was the Technical Director for Force Projection and Maneuver Support. The Deputy Director of ERDC-CRREL was Mr. David B. Ringelberg, and the Director was Dr. Joseph L. Corriveau.

COL Teresa A. Schlosser was Commander of ERDC, and Dr. David W. Pittman was the Director.

Acronyms and Abbreviations

AASHTO	American Association of State Highway and Transportation Officials
AC	Asphalt Cement
ATAF	Asphalt Temperature Adjustment Factor
BCI	Base Curvature Index
CBR	California Bearing Ratio
CRREL	U.S. Army Cold Regions Research and Engineering Laboratory
D_{10}	10% of the Particles are Finer
D_{30}	30% of the Particles are Finer
D_{60}	90% of the Particles are Finer
ELMOD	Evaluation of Moduli and Overlay Design
ERDC	Engineer Research and Development Center
ESAL	Equivalent Single Axle Load
EVA	Ethylene Vinyl Acetate
FDR	Full-Depth Reclamation
FWD	Falling Weight Deflectometer
GSL	Geotechnical and Structures Laboratory
ISM	Impulse Stiffness Modulus
LL	Liquid Limit
LLI	Lower Layer Index
LTPP	Long-Term Pavement Performance
MERRA	Modern-Era Retrospective Analysis for Research and Applications
Mr	Resilient Modulus

NDT	Non-Destructive Testing
NHDOT	New Hampshire Department of Transportation
NMAS	Nominal Maximum Aggregate Size
PG	Performance Graded
PI	Plasticity Index
PL	Plastic Limit
QC	Quality Control
RSME	Root-Mean-Square Error
SBR	Styrene Butadiene Rubber
SBS	Styrene Butadiene Styrene
SCI	Surface Curvature Index
SIP	Structural Index of Pavement
SM	Silty Sand
SN	Structural Number
SNC	Modified Structural Number
SN_{eff}	Effective Structural Number
SP	Poorly Graded Sand
USCS	United Soil Classification System

Unit Conversion Factors

Multiply	By	To Obtain
British thermal units (International Table)	1,055.056	joules
degrees (angle)	0.01745329	radians
degrees Fahrenheit	(F-32)/1.8	degrees Celsius
feet	0.3048	meters
gallons (U.S. liquid)	3.785412 E-03	cubic meters
inches	0.0254	meters
mils	0.0254	millimeters
pounds (force) per square inch	6.894757	kilopascals
pounds (force) per square inch	0.00689476	megapascal
pounds (mass)	0.45359237	kilograms
square yards	0.8361274	square meters
tons (2,000 pounds, mass)	907.1847	kilograms
yards	0.9144	meters

1 Introduction

1.1 Background

Asphalt materials as pavements experience significant distresses, both traffic and environment related, throughout their service life. To properly design for the range of distresses, asphalt materials are frequently modified with new, innovative materials to increase the mechanical performance and to decrease life-cycle costs. One of the most common modifications is the use of polymers, which are typically added to asphalt binders. In this context, they are known as liquid polymers as they are dispersed in the liquid asphalt binder. Polymers have seen significant use and have been proven to improve asphalt performance. This includes increased stiffness at high temperatures to prevent rutting, increased flexibility at intermediate temperatures to minimize fatigue cracking, and decreased brittleness at low temperatures to prevent low-temperature thermal cracking and frost-heave related cracking. Polymer modification is particularly useful in cold regions as it allows the use of a soft base binder to prevent thermal cracking while maintaining significant amounts of stiffness at high temperatures to prevent rutting. This would be challenging for an unmodified binder as a binder that is sufficiently soft to prevent low-temperature thermal cracking will likely experience significant rutting at high temperatures.

The usage of polymeric materials in asphalt is not a new concept. It has been used in one way or another since latex modification was introduced in the 1930s in Europe and the 1950s in the United States (King et al. 1999). Modern polymers were first used by European contractors and later integrated by contractors in the United States (Brûlé 1996; Collins 1995). The most common types of polymers used in asphalt were styrene butadiene styrene (SBS), butadiene rubber (SBR), and ethyl-vinyl acetate (EVA). These three remain the most popular forms of polymer modification in the current asphalt industry.

Some of the benefits of polymer modification are higher elastic recovery, higher softening point, higher viscosity at high temperatures, higher fracture energy, higher cohesive strength, and higher ductility measured on asphalt binders, as well as greater resistance to rutting, fatigue cracking, and low-temperature thermal cracking on asphalt mixtures (Bates and Worch 1987).

Numerous studies have evaluated the effectiveness of polymers in both asphalt binders and asphalt mixtures. Currently, the consensus in the field is that these additives are effective ways to improve asphalt mechanical properties and to increase its resistance to distresses. Studies have shown that polymer-modified materials increase the fatigue resistance of asphalt by increasing stiffness and elastic recovery of materials. Newman (2003) investigated the effectiveness of using SBS and SBR in airfield mixtures and evaluated the performance of these materials using the bending beam fatigue test. The results of that study showed significant increases in cycles to failure for the modified materials. The improvement in fatigue properties has led other researchers to propose polymer-modified materials as part of a perpetual pavement design, where the strain at the bottom of the asphalt layer never exceeds the materials endurance limit (Newcomb 2003).

Another area where polymers can improve asphalt mixture performance is with respect to low-temperature thermal cracking. This improvement is typically achieved by increasing the amount of energy required to fully fracture the material rather than the conventional thinking of decreasing stiffness and brittleness. Isacsson and Zeng (1998) investigated five different polymer-modified materials in three asphalt-mix designs using the thermal restrained specimen test. The results of the study showed that, while the effectiveness of the different polymers heavily depended on the specific polymer as well as aging and mixture volumetrics, all of the polymer materials improved the resistance to low-temperature thermal cracking (Isacsson and Zeng 1998). This was most apparent through the fracture-strength parameter rather than the critical fracture temperature parameter.

While polymers have significant performance benefits when used with asphalt materials, they are not without their challenges. One of the most prominent ones is storage and handling of the material. When polymers are blended with asphalt binder, they form long networks of polymer chains. These chains become suspended in the binder as a heterogeneous mixture. Also known as crosslinking, this allows the polymers to act as a unit, which is ultimately responsible for improving the asphalt material's performance. Disturbing or destroying this polymer network significantly reduces the performance gains of the material (Wegan 2001). Preventing this requires specialized heating and storage tanks. While these are commonly available in the continental United States as part of routine asphalt construction, this equipment is not typically available in remote environments where temporary plants are more common.

To combat this issue, recent work has led to the development of solid polymers (Azam et al. 2019). Solid polymers are introduced into the pug mill or drum mixer at an asphalt plant rather than being mixed into the binder beforehand. Because of the dry-mixing process these undergo, no specialized equipment is needed to integrate the materials into normal production procedures. Another advantage of solid polymers is that they can be stored dry in pallets, bags, or containers so that they are always available and ready for quick deployment in remote regions. Because there has been limited laboratory and full-scale research on solid polymers, there is not a clear consensus on the performance impacts of these materials for pavements in cold regions. The effects of extended low temperatures, severe daily temperature cycling, and freeze–thaw effects are much different than those seen in temperate climates where polymers are more commonly used. Some work has investigated the effect of solid polymers on the high-temperature properties of asphalt binder, mixture indirect tensile strength, and mixture moisture susceptibility, which generally showed promising results in the laboratory (Azam et al. 2019). However, it appears that no studies have looked at the low temperature properties (linear viscoelastic and fracture) and long-term field performance of mixtures modified with solid polymers.

Researchers at the U.S. Army Engineer Research and Development Center's Cold Regions Research and Engineering Laboratory (ERDC-CRREL) were tasked with this investigation as part of the "Innovative Construction Materials for Cold Regions" research program. In recent years, the Army has been pushing to expand cold region infrastructure construction capabilities and to expand the durability of said infrastructure. Cold climates present unique challenges to using asphalt materials, and the use of solid polymers offers a number of qualities that can potentially address these challenges. The ultimate goal of this study, and for the program, is to investigate solutions for the Army that can provide superior-performing pavements in cold regions.

1.2 Objective

The objective of this project was to evaluate the feasibility and benefits of using a solid polymer as an additive to the asphalt layer to mitigate the multitude of distresses in cold regions. The polymer material chosen for this study was Superplast, a solid, pelletized polymer material produced by

Iterchimica. This study extensively investigated the production, construction, and the structural performance of the modified asphalt mixtures in both the laboratory and the field.

1.3 Approach

This study conducted several tasks to better investigate the impact of solid polymer on the performance of asphalt pavements, which, if found feasible, ultimately could assist practitioners with integrating and using solid-polymer-modified mixtures. The following steps outline the scope of this study:

1. Establish a pavement site in a cold climate for field evaluation.
2. Produce solid-polymer-modified mixtures and construct them in the field using conventional construction practices and equipment.
3. Sample material from the production and conduct a comprehensive laboratory evaluation to quantify the impacts of the additive on the performance of the asphalt material under different testing conditions.
4. Field test the constructed sections over time to understand the initial performance of the modified section and how that performance changes over time due to traffic and environmental damage.
5. Take core samples from the field for forensic investigations to further quantify the changes in the performance of these materials over time.

This report presents the first phase of this project, which covers steps 1, 2, and part of 4. The main goal of this phase was to produce the polymer-modified asphalt mixtures, to use the mixtures as an asphalt layer in an actual roadway, and to conduct initial field testing on these layers to better understand the impacts of the solid polymers on the pavement performance. This phase of the project ran from September 2018 to September 2019.

This report aims to advance the current understanding of the impact of solid polymer on the structural performance and capacity of pavements. Following this introduction to the problem and objectives, section 2 discusses the selection and evaluation of the project site, production of the modified mixtures, and the construction of these materials. Section 3 explores the initial field evaluation of the project sections with in situ load testing. Section 4 presents a preliminary life cycle cost analysis. Section 5 summarizes the findings and conclusions of this report and recommends follow-on work.

2 Site Evaluation, Material Production, and Pavement Construction

This section describes the test-site conditions and evaluation as well as the production and construction of the solid-polymer-modified mixtures at the site.

2.1 Site description and evaluation

2.1.1 General site conditions

The roadway selected for this study (GPS 43.391382, −72.210508) is in Newport, New Hampshire. This section is on Corbin road on the west-bound side of State Route 10, serving mostly residential and some truck traffic. The original roadway was constructed in 1990 and was rehabilitated in 2000 with an unstabilized, full-depth reclamation (FDR). This was then surfaced with 3 in. (75 mm) of a 12.5 mm nominal maximum aggregate size (NMAS) asphalt surface layer, which is how the roadway remains today. Figure 1 shows a cross section of the roadway while Figure 2 provides a satellite image of the site.

Figure 1. Corbin Road pavement cross section.

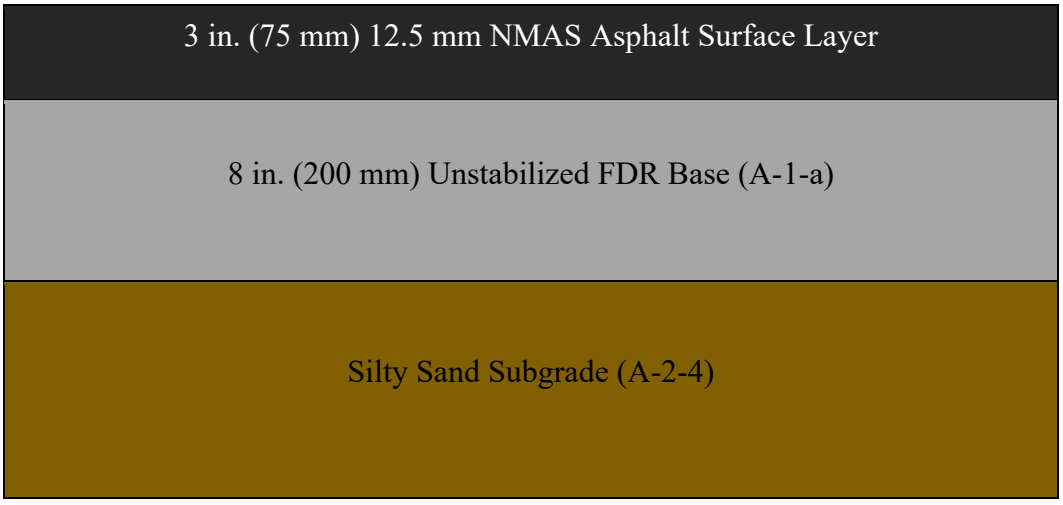

Figure 2. Corbin Road test section satellite image.

The climate of the area is typical for northern New England. Summers have average high temperatures of 30°C with moderate amounts of precipitation, while winter temperatures can be as low as –34°C with 30 to 60 annual freeze–thaw cycles. Table 1 summarizes the relevant pavement climate information from the Long Term Pavement Performance (LTPP) climate tool using the Modern-Era Retrospective Analysis for Research and Applications (MERRA) database (Federal Highway Administration 2016b).

Table 1. Corbin Road climatic data.

Lowest Yearly Air Temperature	–37.0°C
Low Pavement Temperature 50%[a]	–27.0°C
Low Pavement Temperature 98%	–33.80°C
High Avg. Pavement Temperature of 7 Days 50%	50.16°C
High Avg. Pavement Temperature of 7 Days 98%	53.78°C

Researchers from CRREL worked with the Newport Department of Public Works to coordinate the production and construction of the test section: a 2 in. (50 mm) asphalt overlay on the existing roadway. The Town of Newport was to seal and repair the existing distresses in the section, further described in subsequent paragraphs, prior to construction.

2.1.2 Subgrade soil

Particle-size analysis tests were conducted on soil samples collected from the site and tested in accordance with ASTM (2017c) D6913M-17, *Standard Test Methods for Particle-Size Distribution (Gradation) of Soils Using Sieve Analysis*. Atterberg limits tests (i.e., liquid limit (LL), plastic limit (PL), and plasticity index (PI)) were performed following ASTM (2017b) D4318-17e1, *Standard Test Methods for Liquid Limit, Plastic*

Limit, and Plasticity Index of Soils. Figure 3 shows the particle-size distribution curve of the presented soil. Based on these results, the soil was classified as SM (silty sand) according to the Unified Soil Classification System (USCS) and A-2-4 according to the American Association of State Highway and Transportation Officials (AASHTO) classification system.

Figure 3. Site soil grain-size distribution curve.

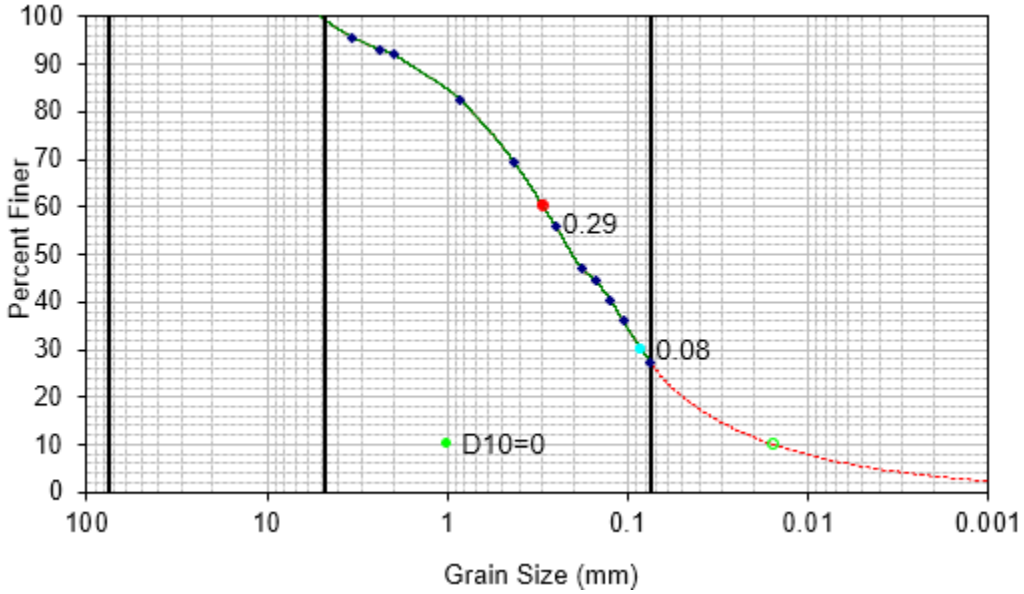

The grain-size distribution curve was analyzed by using different particle sizes (D_{60}, D_{30}, and D_{10}) to better classify the subgrade soil. As Figure 3 shows, D_{10} is 0.015 mm, which means that 10% of the particle are finer and 90% are coarser than 0.015 mm. Here, D_{30} is 0.084 mm and D_{60} is 0.293 mm, which means 30% and 60% of the particle are finer and 70% and 40% are coarser than 0.084 mm and 0.293 mm, respectively.

To determine the measures of soil gradation (i.e., well graded or poorly graded), the uniformity coefficient (C_u) and the coefficient of gradation (C_c) were determined from Figure 3. C_u is defined as the ratio of D_{60} to D_{10}. When C_u is greater than 6, the soil is classified as well graded. The value of C_c must be between 1 and 3 to classify as well-graded soil. For this soil, C_u is 18.97 and C_c is 1.55. Based on these results, the soil is well-graded soil.

A standard proctor test was conducted on soil collected in the field in accordance to ASTM (2012) D698-12e12, *Standard Test Methods for Laboratory Compaction Characteristics of Soil Using Standard Effort (12 400 ft-lbf/ft³ (600 kN-m/m³))*, to determine the optimum moisture content

and maximum dry density of the soil. Figure 4 shows the proctor compaction curve for the silty sand soil. As seen in Figure 4, the optimum moisture content (W_{opt}) is 10%, and the maximum dry density ($\gamma_{dry\ max}$) is 1.869 gm/cm^3.

Figure 4. Site soil proctor compaction curve.

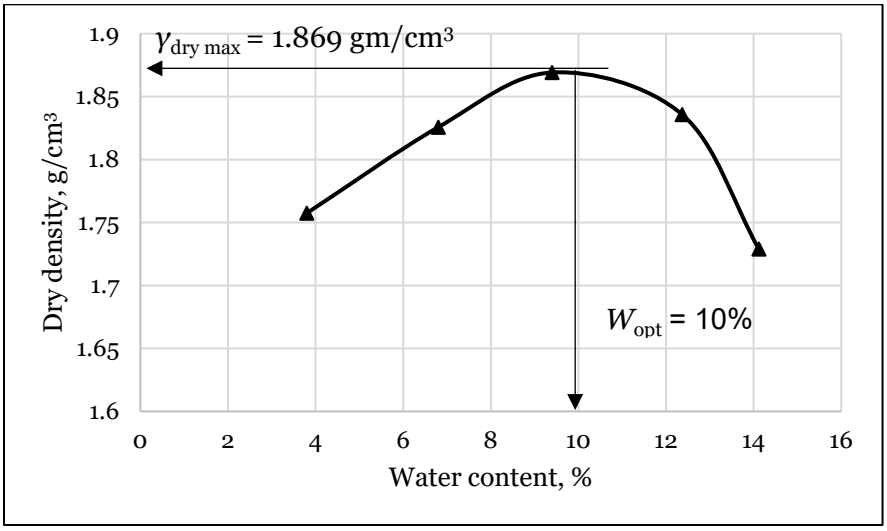

The correlation between strength and stiffness of unbound materials and physical soil index was used to estimate the California bearing ratio (CBR) and resilience modulus (Mr) of the soil at optimum moisture content (Witczak et al. 2000). The CBR values were obtained from the soil index in equation (1).

$$\mathrm{CBR} = \frac{75}{1+0.728(\mathrm{WPI})}, \tag{1}$$

where

WPI = percent of passing #200 sieve × plasticity index.

The resilient modulus of unbound materials in equation (2) was used to estimate the stiffness of the soil layer:

$$\mathrm{Mr} = 2555(\mathrm{CBR})^{0.64}. \tag{2}$$

Table 2 shows the measured soil properties and the calculated CBR and Mr determined from the above equations.

Table 2. Physical properties of the site soil.

Soil Type	P#200[a]	LL	PI	G_s[b]	$\gamma_{dry\ max}$ (gm/cm³)	W_{opt} %	CBR	Mr (psi/MPa)
A-2-4 (SM)	27.43	25.5	1.4	2.684	1.869	9.5	58	35000/ 241.3

[a] Percent passing the #200 sieve.

[b] Specific gravity.

Note that the aforementioned models (i.e., equations [1] and [2]) were used to determine seed values of the soil layer for backcalculation (discussed in section 3.3.3) and to get a general idea of the soil stiffness. Laboratory testing is necessary if these values are needed as input parameters for pavement design and evaluation.

2.1.3 Base course layer

The existing base course layer is composed of material from a previous unstabilized full-depth reclamation project. Unstabilized full-depth reclamation rehabilitates an old, distressed pavement by milling the existing asphalt layer and mixing it with the base or subgrade beneath. The *unstabilized* refers to how these practices do not incorporate any additives, such as cement, lime, ash, asphalt emulsion, or foamed asphalt, to strengthen the base material. When compared to AASHTO soil classification, unstabilized FDR is like an A-1-a and A-1-b in terms of mechanical properties and structural response. Figure 5 shows the grain-size distribution of this FDR material.

Figure 5. Grain-size distribution curve of the base layer.

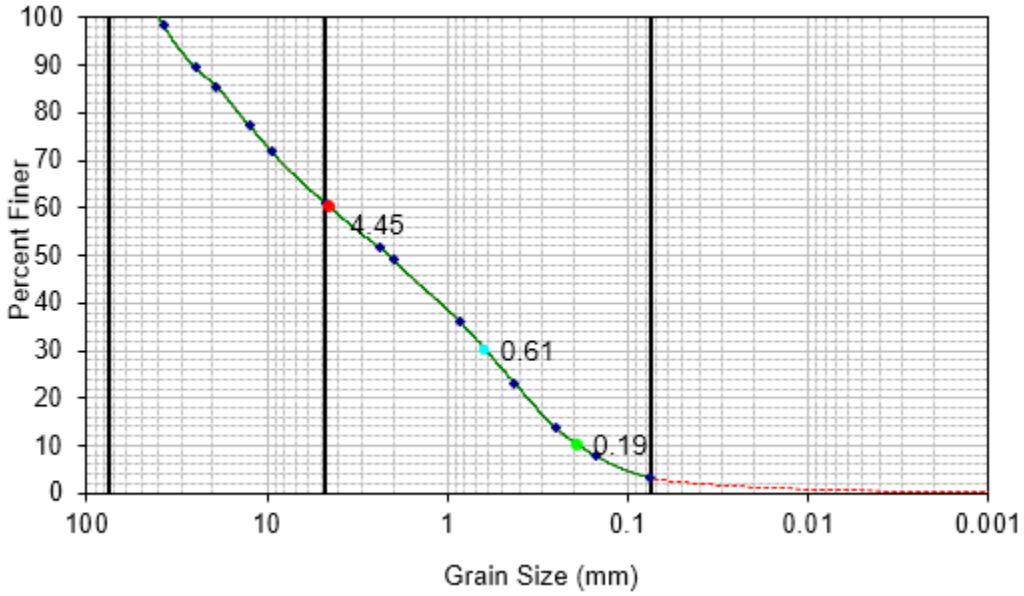

The grain-size distribution curve of base layer was analyzed by using particle sizes: D_{60}, D_{30}, and D_{10}. Figure 5 shows, D_{10} is 0.187 mm, D_{30} is 0.609 mm, and D_{60} is 4.448 mm. The uniformity coefficient (C_u) and the coefficient of gradation (C_c) were determined from Figure 5 to find the measures of the gradation. For this base layer, C_u is 23.83 and C_c is 0.45. As Figure 5 shows, more than 50% passes the #4 sieve and less than 5% passes the #200 sieve. According to the USCS, this soil is poorly graded sand, gravelly sand, little or no fines (SP). According to the AASHTO classification system, this soil classified as an A-1-a.

2.1.4 Existing asphalt layer

The existing pavement at the Corbin Road site is surfaced with a 3 in. asphalt layer. This layer, approximately 15 years old, is a 12.5 mm NMAS performance graded (PG) 64-22 mixture designed to meet the New Hampshire Department of Transportation (NHDOT) specifications. Before the construction of the test-section overlays, the research team conducted a distress survey to characterize the existing condition of the asphalt layer. The distress survey followed guidelines from the Federal Highway Administration LTPP program (Miller and Bellinger 2014). Using the survey information will help contextualize the long-term performance of the overlay sections as the existing asphalt layer beneath them will have a significant impact on their performance.

For the survey, the distresses were initially marked off by a reference location. After construction was complete and the section limits were determined and marked off, the distress survey was reformatted to line up with the four constructed sections. Table 3 shows a general overview of the results from the distress survey.

Looking at the distress survey, it is evident that transverse cracking was the most prominent distress in the existing pavement. Transverse cracking, also known as low-temperature cracking, is caused primarily by extreme cooling events. During cooling events, the asphalt surface layer attempts to contract but is restricted by friction with the base layer underneath. Because of this restraint, thermal stresses accumulate in the layer. If these stresses accumulate to a point where the internal stresses are higher than the tensile strength of the material, cracks will form.

Table 3. Corbin road distress survey results.

Distress	Measure	Section			
		1 (Control)	2 (5% Polymer)	3 (7.5% Polymer)	4 (2.5% Polymer)
Transverse Cracking	Average Crack Spacing (m)	8.2	6.2	7.6	5.9
	Crack Length per 500 m (m)	185.7	233.3	194.4	228.6
	Average Crack Width (mm)	25	21.8	28.1	25
	Severity	High	High	High	High
Fatigue Cracking	Lane Area Cracked (%)	0	2.5	5	5
	Severity	NA	Low	Low-Moderate	Moderate
Rutting	Max Depth (mm)	0	0	0	0

Considering that the original asphalt layer used a PG 64-22 binder and the pavement is highly aged (15+ years old), it is not surprising to see high amounts of high-severity transverse and thermal cracking. The winter climate for Newport, New Hampshire, which can experience annual low temperatures around –30°C, requires a PG XX-28 binder to meet the minimum 50% reliability temperature according to LTPP (Federal Highway Administration 2016a). In addition, the existing pavement has been in service for more than 10 years, which likely has significantly aged the material. This aged material, which will be more brittle than new materials, is more susceptible to cracking.

When comparing the four sections, their performance with respect to transverse cracking is generally similar. Section 1 (which the control was built upon) and 3 (7.5% polymer) have slightly higher amounts of thermal cracking and lower average spacing than section 2 (5% polymer) and 4 (2.5% polymer). Figure 6 and Figure 7 show some examples of high severity thermal cracking on the sections.

Figure 6. Corbin Road thermal cracking example in section 2.

Figure 7. Corbin Road thermal cracking example in section 4.

Beyond the transverse cracks, the only other prominent distress in the sections was areas of low- and moderate-severity fatigue cracking in section 2 (5%polymer), section 3 (7.5% polymer), and section 4 (2.5% polymer). The areas of fatigue cracking were localized to the wheel path and were generally 1–2 ft (30–60 cm) wide with no evidence of potholing, delamination, pumping, or other types of consequent deterioration observed in the fatigued areas. Comparing the sections, section 3 (7.5% polymer) and section 4 (2.5% polymer) had most of the moderate severity fatigue cracking area while section 2 (5% polymer) had only low-severity fatigue cracking. Section 1 (control) showed no evidence of fatigue cracking. Figure 8 shows an example of the wheel path fatigue cracking seen on the section.

Figure 8. Corbin Road fatigue cracking example in section 4.

Looking at the third major distress in asphalt pavements, rutting, there was no significant evidence of rut development in any of the sections. As a check, the team placed a 48 in. (122 cm) steel beam across the wheel path four times per section and measured the rut depth with a straight edge. In each case, no measurable rut depth was observed. This finding, combined with the relatively minor amounts of fatigue cracking, suggests that the Corbin Road pavement does not have structural problems in its current state. This is not entirely surprising considering that Corbin road is a low-volume road with minimal heavy traffic. As evidenced by the high-severity thermal cracks and a significant amount of surface weathering and degradation, environmental distresses are the prevailing type of distresses for this section.

2.2 Production and construction of the asphalt overlay layer

2.2.1 Material production

To produce the asphalt mixtures for the field sections, a locally available plant mix was selected as the control mixture to modify with the solid-polymer additives. Pike Industries produced the control mixture at their batch plant in Newport, New Hampshire: a 12.5 mm NMAS Superpave mix design produced with a PG 64-22 binder. This mixture was composed of four stockpiles: a 1/2 in. (12.5 mm) crushed gravel, a 3/8 in. (9.5 mm) crushed gravel, a washed sand, and a manufactured sand. Table 4 lists the stockpile gradations, gravimetric properties, and proportions used in the mixture. Figure 9 and Table 5 provide the design gradation and other volumetric properties of the control mixture. Note that the mixture chosen for this study was a virgin mixture that did not contain any recycled asphalt pavement. This limited the variability of the mixtures, allowing the effect of the solid polymers to be more closely analyzed.

Table 4. Mixture aggregate stockpile proportions.

Aggregate Stockpile		1/2 in. Crushed Gravel	3/8 in. Crushed Gravel	Washed Sand	Manufactured Sand	Mixture Blend
Percent in Blend		21	37	19	23	100
Percent Passing (%)	3/4 in. / 19.0 mm	100.0	100.0	100.0	100.0	100.0
	1/2 in. / 12.5 mm	84.6	100.0	100.0	100.0	96.8
	3/8 in. / 9.5 mm	22.4	99.7	100.0	100.0	83.6
	#4 / 4.75 mm	2.9	45.3	99.6	81.6	55.1
	#8 / 2.36 mm	1.7	9.9	85.7	64.1	35.0
	#16 /1.18 mm	1.5	4.6	60.2	47.9	24.4
	#30 /0.60 mm	1.4	3.1	41.2	36.9	17.8
	#50 / 0.30 mm	1.3	2.1	20.1	23.0	10.1
	#100 / 0.15 mm	1.1	1.3	5.8	11.9	6.0
	#200 / 0.075 mm	0.9	0.9	2.7	8.7	3.0
Bulk Specific Gravity		2.857	2.651	2.525	2.553	2.643
Apparent Specific Gravity		2.893	2.719	2.558	2.579	2.688
Water Absorption (%)		0.67	1.52	0.52	0.40	0.90

Figure 9. Design gradation curve for the 12.5 mm control mixture.

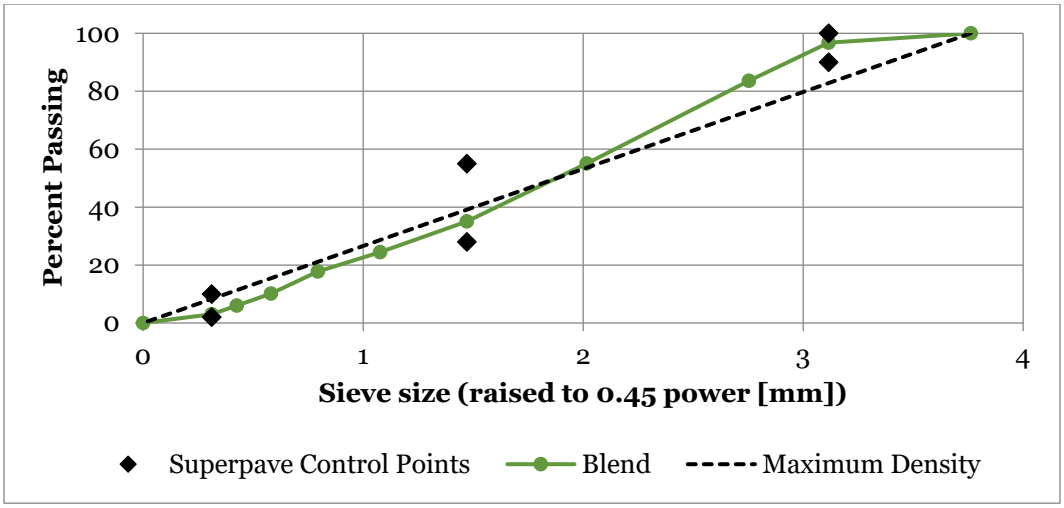

Table 5. Mixture design properties.

Design Property		Control Mixture Design Values	NHDOT/Superpave Spec. Limit	Applicable Standard
NMAS (mm)		12.5	-	-
Design Traffic (ESALs[a])		> 0.3 million	> 0.3 million	AASHTO M323
Design Gyrations		50	50	AASHTO M323
PG Grade of Binder		64-22	-	AASHTO M320
Percent Passing (%)	3/4 in. / 19.0 mm	100.0	100	-
	1/2 in. / 12.5 mm	96.8	90-100	-
	3/8 in. / 9.5 mm	83.6	-	-
	#4 / 4.75 mm	55.1	-	-
	#8 / 2.36 mm	35.0	58-28	-
	#16 /1.18 mm	24.4	-	-
	#30 /0.60 mm	17.8	-	-
	#50 / 0.30 mm	10.1	-	-
	#100 / 0.15 mm	6.0	-	-
	#200 / 0.075 mm	3.0	2-10	-
Binder Content (%)		5.8	-	-
Effective Binder Content (%)		4.5	-	-
Bulk Specific Gravity at Design Gyrations		2.386	-	ASTM D2726
Air Voids at Design Gyrations (%)		4.0	4	ASTM D2726
Maximum Specific Gravity		2.492	-	ASTM D2041
Bulk Specific Gravity of Aggregate		2.643	-	ASTM C127/128
Voids in Mineral Aggregate (%)		14.5	< 14.0	AASHTO M323
Voids Filled with Asphalt (%)		73.8	70-80	AASHTO M323
Dust-to-Binder Ratio		0.68	0.6-1.2	AASHTO M323

[a] Equivalent single axle load.

For two reasons, this study chose to produce the mixture for the test sections at a batch plant. First, batch plants run in discrete increments where the amount of material placed into the pugmill mixer can be readily controlled (as compared to a continuous flow drum plant), allowing more precise control of the aggregate and solid-polymer amounts in each batch. Second, the test sections in this study (360 × 8 m) required a relatively small amount of material (compared to conventional road construction), which is easier to accomplish with a small batch plant. Figure 10 shows the batch plant used in this study.

Figure 10. The batch plant used to produce the study mixtures.

The test section plan included constructing four sections. One section consisted of the control mixture previously discussed while the other three consisted of solid-polymer-modified sections with 2.5%, 5.0%, and 7.5% solid polymer by weight of binder. The control mixture was produced using standard procedures as it is a mixture the plant produces regularly. The modified mixtures required some changes to the usual practice to be properly produced.

For the solid-polymer-mixture production, this study used a dry process. Essentially, this means that the polymers are added directly to the pug mill mixer when the aggregate is being mixed but the heated asphalt binder has not been introduced. The intent of this, per the manufacturer's recommendations, is to allow time for the polymers to break down from the heat of the hot aggregate, which allows the polymer to evenly disperse before the

heated binder is introduced into the mix. Specifically, this study used the following to add the polymers:

1. Combine the aggregate stockpiles in the normal proportions as for the control mix.
2. Set the temperature of the drying drum so that the aggregate temperature is between 170°C and 180°C. This temperature facilitates the breakdown and dispersion of the polymer.
3. Allow the pug mill to mix the aggregate for a minimum of 15 seconds to ensure uniform aggregate distribution.
4. Introduce the solid-polymer pellets into the pug mill with the hot aggregate. Using a feed hopper is the easiest method for this. Continue to mix for 15 seconds to allow the polymer to break down and disperse.
5. Introduce the heated binder into the pug mill. Allow a minimum of 30 seconds to mix in the asphalt binder. The binder should be heated to normal mixing temperatures.
6. Add any additional fines if they are being used (such as baghouse fines), and allow an additional 30 seconds of mixing.
7. Drop the mix out of the pug mill and start the process over again for the next batch.

In a normal, large-scale production plant, the solid-polymer pellets would be added using a hopper that feeds directly into the pug mill (in the case of a batch plant). For this study, however, the smaller scale of the work required some modifications. Since purchasing a hopper was not feasible for such a small project, the solid polymers were manually added to the pug mill through the side access door after the aggregates had been mixed for 15 seconds. The solid-polymer dose was controlled by filling meltable plastic bags with approximately 9 lb (4.1 kg) of polymer. Each bag of polymer provided a dosage of 2.5% by weight of binder for a 3-ton (2720 kg) batch of mix. For the 5.0% and 7.5% mixes, two and three bags were added respectively to provide the correct dosage. For reference, Figure 11 shows a close-up view of the solid polymers used and the polymer stored in the meltable bags at the plant prior to production. Table 6 lists the physical properties of the polymers used in this study.

On the day of production, the mixes were produced in 3-ton (2720 kg) batches using the process described above. Typically, it took about seven batches to fill a truck with asphalt. To supply enough mix for each section, four trucks were needed per section. The first mix manufactured

was the control, then the 5.0% polymer, the 7.5% polymer, and the 2.5% polymer last.

Figure 11. Solid-polymer pellets close-up view (*left*) and packaged in meltable bags for production (*right*).

Table 6. Solid-polymer physical properties.

Physical Property	Value
Pellet Diameter (mm)	3.0–4.0
Pellet Thickness (mm)	0.75–1.25
Softening Point (°C)	160–180
Bulk Specific Gravity	0.4–0.6
Pellet Specific Gravity	0.7–0.8

As a check to the consistency of the mixture production, one bucket of asphalt mixture was sampled from each truck before it left for the construction site. Each of these buckets was tested for gradation per ASTM (2017c) D6913-17, asphalt content per ASTM (2017a) D2172, and volumetric properties with a gyratory compactor per ASTM (2019b) D2726. Table 7 shows the results from these quality control tests.

Looking closely at the results, there is generally little variation between the mixture properties. Looking at the gradations first, all four mixtures have similar distributions of particle sizes that match well with the design gradation. One slight exception to this observation is the #100 and #200 sieve sizes, which are consistently lower than the design gradation. Generally, fine particles act as fillers as part of the asphalt binder mastic (binder plus fines). Lowering the amount of fines in the mastic can result in lower stiffness and a mixture that is prone to bleeding (flushing of liquid binder to

the surface, leaving a thin film of asphalt), hence why the dust-to-binder ratio is a requirement in Superpave specifications. While these signs of bleeding were not noticed during construction, it is worth noting for later analysis.

Table 7. Production quality control results.

Mixture		Design Gradation	Control QC[a] Test	2.5% Polymer QC Test	5.0% Polymer QC Test	7.5% Polymer QC Test
Percent Passing (%)	3/4 in. / 19.0 mm	100.0	100.0	100.0	100.0	100.0
	1/2 in. / 12.5 mm	96.8	95.8	96.0	95.9	96.0
	3/8 in. / 9.5 mm	83.6	84.2	83.6	85.9	85.3
	#4 / 4.75 mm	55.1	52.1	50.4	54.6	50.1
	#8 / 2.36 mm	35.0	36.5	33.6	39.8	34.8
	#16 /1.18 mm	24.4	27.6	24.8	30.1	25.5
	#30 /0.60 mm	17.8	19.0	17.1	19.9	17.0
	#50 / 0.30 mm	10.1	10.1	9.1	9.6	9.7
	#100 / 0.15 mm	6.0	4.8	4.3	3.8	5.0
	#200 / 0.075 mm	3.0	2.8	2.4	2.4	3.0
Binder Content (%)		5.80	5.79	5.92	5.89	6.12
Air Voids at 50 Gyrations (%)		4.0	4.3	3.3	4.2	3.2
Maximum Specific Gravity		2.492	2.497	2.482	2.487	2.485
Voids in Mineral Aggregate (%)[b]		14.5	14.8	14.6	15	14.6
Voids Filled with Asphalt (%)[c]		73.8	70.9	77.2	72.4	77.8
Dust-to-Binder Ratio		0.68	0.63	0.51	0.52	0.63

[a] Quality control.

[b] Minimum Superpave voids in mineral aggregate for 12.5 mm NMAS mix is 14.0.

[c] Allowable Superpave voids filled with asphalt range for 12.5 mm NMAS mix is 70–80.

The volumetric results show the same general trend of similarity between the mixtures. As mentioned with the lower amount of fines in the gradations, the corresponding dust-to-binder ratios are consistently lower than the design value. The 2.5% and 5.0% mixtures fell to a ratio below 0.60 (i.e., 0.51), failing the Superpave requirements of 0.60 to 1.20. No signs of bleeding were seen during the construction to suggest this was a concern. Looking at the measured air voids, the control and 5.0% mixes fall within the 4.0% ± 0.5% tolerance allowed by Superpave specifications. On the other hand, the 2.5% and 7.5% mixtures fall below this range. Looking at the binder results, these two have the highest binder content. Higher binder contents generally allow easier compaction, which will lower the

design air voids, partially explaining the results seen here. One other property worth noting is the maximum specific gravity results. All three polymer mixes were measured to have specific gravities approximately 0.100 lower than to the control mixture. This is caused by, all things being equal, the addition of polymers as they have lower specific gravity than the components of the mixture, lowering the overall specific gravity of the mixture.

Overall, the quality control results show that the four mixtures produced were generally similar in composition and volumetric properties. The properties that do have slight deviations, such as dust-to-binder ratio, percent binder, and air voids, should be kept in mind during the analysis of the mixtures as these differences could explain some of the observed differences in mechanical properties and field performance.

As a general observation, there were no significant challenges producing the solid-polymer-modified mixtures. With the temperature used during production, all the polymers appeared to break down and disperse in the mix as expected. Upon inspecting the loose mix, there were no signs of clumping or unmixed polymers present. While the mixing process used in this study was more highly controlled than typical construction practices, there are no anticipated issues with other production facilities integrating these additives into various other asphalt mixtures. Further investigation is still needed to determine whether the solid polymer is fully dissolved in the asphalt mixture or not.

2.2.2 Test section construction

The four test sections at the Corbin Road site were constructed on 12 June 2019. The weather was sunny and clear with a high temperature of 29°C The day prior to construction, approximately 15 m of roadway at the end of the sections was milled to allow a smooth transition to the existing road, the existing cracks in the section were sealed, and the section was swept clean of debris.

The planned order of construction was first to pave the control lane followed by the 5.0% lane, which were consecutive lanes. After the 5.0% lane was finished, the contractor moved the equipment back to the start of the section and paved the 7.5% lane followed by the 2.5% lane. Each section had a 30 m buffer zone between it and the companion section to prevent areas of mixed materials being analyzed. Figure 12 provides a general schematic of the lane setup.

Figure 12. Corbin Road test section layout.

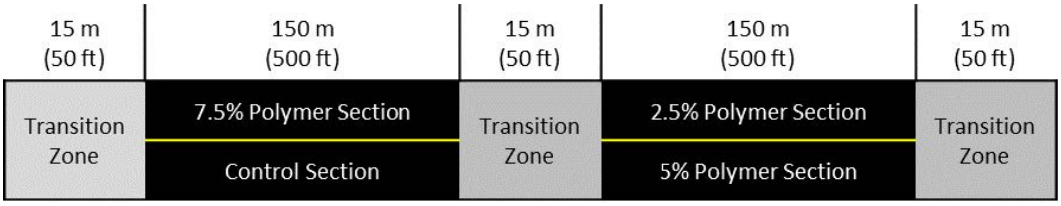

Prior to the paving of each lane, an RS-1 rapid setting emulsion was applied as a tack coat on the existing asphalt layer. The application rate for the tack coat was 0.20 gal./yd^2 (0.90 L/m^2), yielding a residual rate of approximately 0.05 gal./yd^2 (0.225 L/m^2).

The target thickness for the overlay was 2 in., which was constructed in one lift. Each section needed approximately 4 truckloads with a target delivery temperature of 150°C. The construction used a 10-ton paver to lay down the asphalt mat. Next, a 20-ton (18140 kg) steel vibratory roller was used for the breakdown compaction. The vibratory roller's roller pattern was two passes with vibrations at 2400 rpm followed by two static passes. Once breakdown was finished, an 8-ton (7250 kg) steel drum roller was used as the finish roller(Figure 13).

Figure 13. Test section construction on Corbin Road.

During construction, the densities of each section were monitored with an electronic density gauge to understand how each of the mixes compacted under the same compactive effort (Figure 14).

Figure 14. Electronic density gauge.

Densities were measured at eight locations in each section at three different times: first after the paver placed down the mat (screed density), second after the breakdown roller finished its passes (breakdown density), and lastly after the finish roller finished its passes (finish density). The final density of the section was taken the following day after initial trafficking. Figure 15 presents the results from the density measurements. These densities were taken with the intention of comparing the densification of the modified materials to the control. The presented densities were verified against core samples taken after construction and generally showed good agreement.

When adding polymers, one concern related to compaction is that due to the temperature-insensitive nature of the polymers (compared to unmodified binders), the mix may be too stiff to allow proper compaction to occur. The density results show slight differences between the four mixtures at each measuring point, suggesting that this effect was not present for the test sections. For the final densities, the sections reached an average of 94.1%, 93.4%, 94.6%, and 93.8% densities for the control, 2.5%, 5.0%, and 7.5% sections, respectively. All of these met the target density of 93%.

Figure 15. Test section density results.

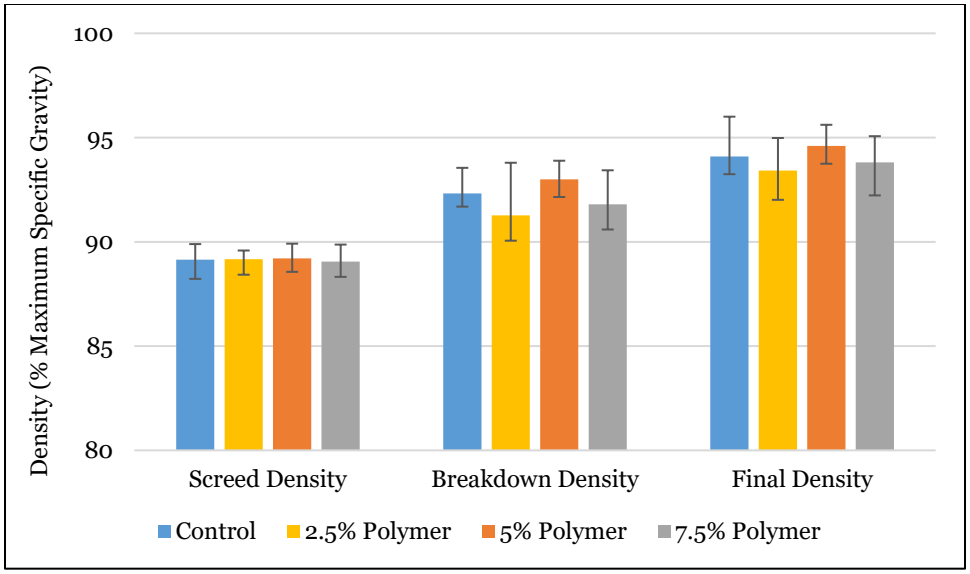

The thickness of the constructed overlay was checked by taking three 6 in. diameter cores of the asphalt layers in each section (Table 8). As the table shows, the control and 5.0% section were appreciably thicker than the 2.5% and 7.5% sections. This information is worth considering when analyzing any structural response of the pavement. All things being equal, thicker pavements are expected to be more structurally sound and durable. The next section further analyzes this.

Table 8. Core thickness results.

Section	Average Thickness (in./cm)	Range (in./cm)
Control	2.08/5.28	1.875–2.25/4.76–5.72
2.5% Polymer	1.86/4.72	1.75–2.10/4.45–5.33
5.0% Polymer	1.99/5.05	1.75–2.15/4.45–5.46
7.5% Polymer	1.59/4.04	1.25–1.90/3.18–4.83

No significant issues were encountered during construction. Throughout the day, the crew observed no major difference between the materials. All sections were reported to have a similar amount of resistance to compaction and workability throughout the day.

During construction, the research team did notice check cracking on the surface. This was most apparent on the 2.5% and 7.5% sections. Check cracking typically occurs when the mix is either compacted when it is too

cool or is over compacted (too much vibratory effort), which ultimately can lead to small, random cracks on the surface (Figure 16).

Figure 16. Check cracking observed in 2.5% polymer sections.

The chosen delivery temperature of 150°C is one potential reason for the development of the check cracks. This temperature was the design compaction temperature of the control mixture. With the addition of polymers, the mix is likely going to significantly stiffen at high temperatures, potentially requiring a higher delivery temperature. The temperature was not increased for the test sections; and the control compaction temperature was used for all the materials. While this partially explains why check cracks were more evident on the 2.5% and 7.5% sections, it does not explain why the check cracks were not seen on the 5.0% section. Another possible explanation is that the amount of compactive effort was too high for the relatively thinner 2.5% and 7.5% polymer sections, although there is no data to support this. Regardless of the observed check cracking during construction, it was much less evident on the section after the finish roller had conducted its passes. After a few days of trafficking, the cracks were essentially invisible, suggesting that the additional compactive effort of traffic closed the cracks slightly. This observation will be important when considering the long-term performance of the section over the next two years.

Overall, the construction of the four sections was mostly without issues or challenges. Looking at the results presented in this section, there is no significant evidence to suggest that the polymer mixes are more challenging to place and compact than the control mixture. The one issue noted, the observance of check cracks in the surface of the 2.5% and 7.5% sections, was not consistent enough across the polymer sections to make any conclusions at this point.

3 Field-Testing Results

The objective of this chapter is to evaluate the performance of the four constructed sections in the field and to investigate the pavement material properties over time.

3.1 Falling weight deflectometer (FWD)

The research team visited the test sections in August 2019 (i.e., 2 months after construction) to conduct in situ testing of the asphalt overlay layers (i.e., one control section and three polymer-modified sections). In situ testing involved FWD testing at different locations in accordance with LTPP protocol (Schmalzer 2006). The team evaluated the load-carrying capacity, obtaining hand auger soil samples in selected areas to determine the soil material properties and measuring temperature in the asphalt layer at four different depths to enhance the interpretation of the FWD results.

FWD testing used a Dynatest 8000 FWD setup with a 300 mm diameter loading plate to monitor the structural integrity of pavements by measuring the deflection of the pavement surface. These deflections are registered by seven transducer sensors (geophones) installed 0, 203, 305, 457, 610, 914, and 1524 mm away from the center of the loading plate (Figure 17). Then, 16 drops are applied at each FWD testing point with four different loads (6000 lbf [26.7 kN], 9000 lbf [40 kN], 12,000 lbf [53.4 kN], 16,000 lbf [71.2 kN]) on the midlane and outer wheel path in both directions of travel in accordance with LTPP protocol (Schmalzer 2006). The number of FWD test points varied from section to section due to the differences in the sections' length. For instance, FWD tests were conducted every 25 ft (7.6 m) for about 500 ft (152 m) in length for sections with no polymer (control), 5% polymer, and 7.5% polymer. For the section with 2.5% polymer, the FWD test was conducted every 20 ft (6 m) for about 250 ft (76 m) in length. The research team used the collected data points from the midlane and outer wheel path in both directions to better evaluate the structural capacity of the investigated sections. The deflection values at each test location were normalized to a 9000 lbf (40 kN) applied force for deflection comparison from different test locations at the same applied contact stress. This load was selected as representative of a typical interstate highway pavement.

Figure 17. Dynatest falling weight deflectometer.

3.2 Temperature gradient and overlay thickness measurements

The thermal gradient through the asphalt surface layer is crucial for the analysis of the FWD deflection data. To address this, two temperature sensors are installed in the FWD device to measure the air and pavement surface temperature during the test. During the FWD deflection, this study measured the temperature gradient by determining the temperature of oil placed in holes drilled from the asphalt surface in the outer wheel path. The holes were drilled to four different depths and tested at 30-minutes intervals as shown in Figure 18. Figure 19 depicts the measured temperature gradient during FWD testing at the outer wheel path (solid lines) and at the midlane (dotted lines).

The depth and the time when the measurements were taken influenced the asphalt temperature readings. For instance, the temperature taken at the mid-depth of the overlay layer always was higher compared to those measured at different depths. As the figure shows, the fluctuations in the temperature gradient between the two sets (i.e., one set measured in the morning and the other set measured in the afternoon) were due to the significant change of the air temperature, which reflect in the pavement temperature.

Figure 18. Layout of measurements of temperature gradients of the pavement surface layer. (AC = asphalt concrete.)

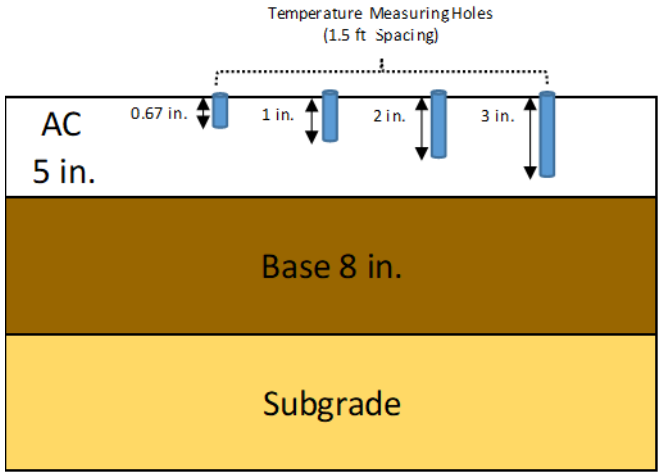

Figure 19. Temperature gradient measurements during FWD testing.

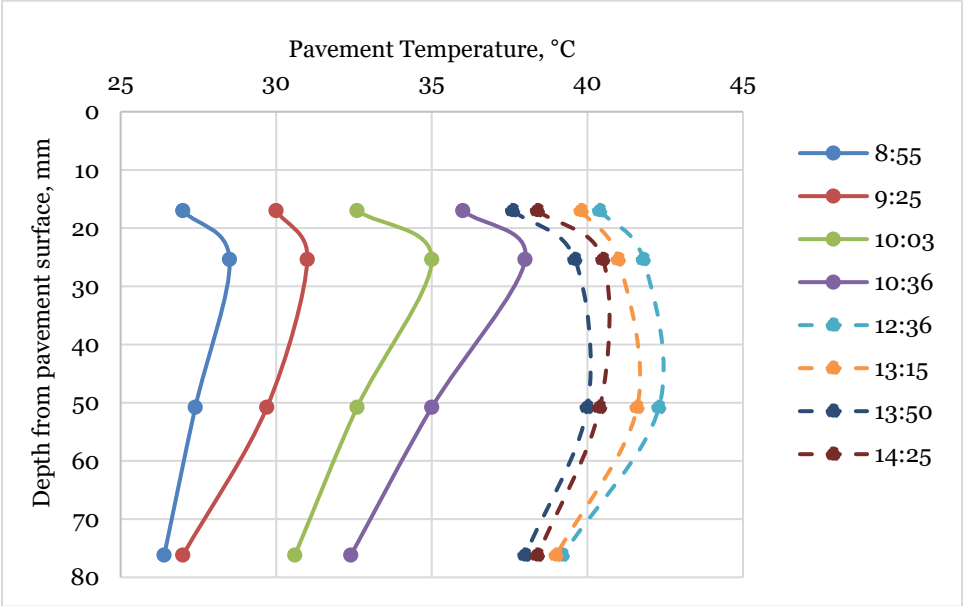

Pavement-layer thickness plays a significant role in backcalculation analysis from FWD deflection data. Therefore, the team obtained several cores from each section to verify the thickness to be used for FWD backcalculation analysis. Figure 20 shows the overlay thickness measurements for each section at 150 ft (45 m) intervals. As Figure 20 shows, the control, 2.5%, and 5% polymer-modified sections have similar asphalt overlay thicknesses. The 7.5% polymer-modified section has the thinnest overlay thickness, averaging approximately 1.65 in. (4.2 cm).

Figure 20. Measured overlay thickness.

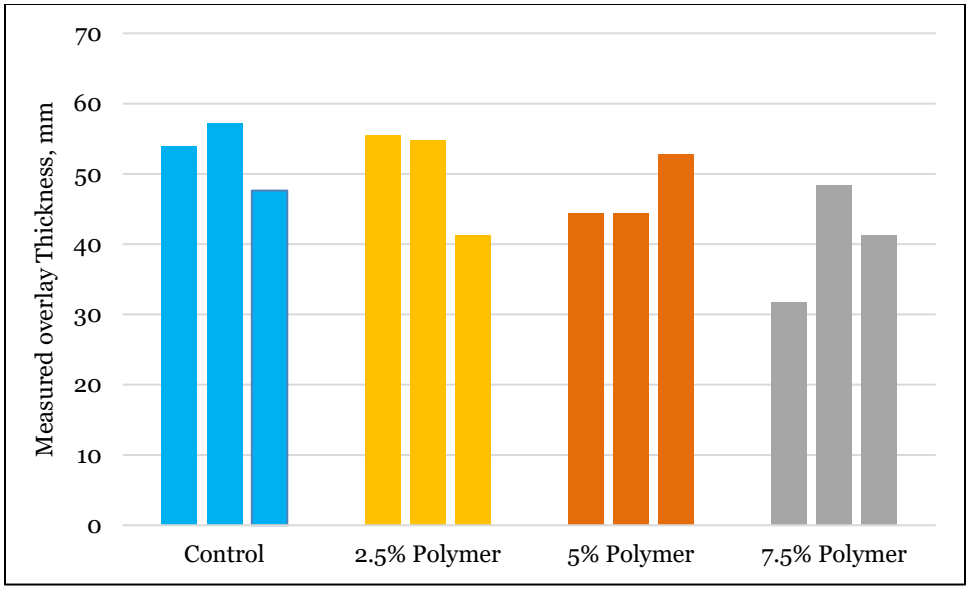

3.3 FWD data analysis and discussion

The pavement-surface-deflection data are a vital tool in evaluating the bearing capacity of pavements. The magnitude and the shape of pavement deflection are a function of many parameters, such as temperature, moisture content, traffic loads, and pavement structure. Thus, caution should be taken during the analysis of FWD data to provide a realistic behavior of pavement structures. As mentioned earlier in this study, FWD testing was conducted to evaluate the structural capacity of polymer-modified sections by measuring the deflection at different load scenarios that simulate the moving traffic. A comprehensive analysis was carried out to interpret the measured FWD deflection at each section to provide a reasonable comparison among the structural capacity of the four sections. The followings methods were used to analyze the FWD deflection data:

1. **First Deflection Sensor (D_0):** The maximum pavement deflection at the load plate reflects the strength of the overall pavement structure. High deflections represent weaker pavement structures and vice versa. Section 3.3.1 discusses in detail the comparison of maximum deflection among four sections.
2. **Deflection Bowl Parameters:** The deflection bowl parameters, such as Surface Curvature Index (SCI), Base Curvature Index (BCI), and Lower Layer Index (LLI) were computed using FWD deflection bowls to better understand the structural capacity of the pavement layers. Section 3.3.2 explains these bowl parameters.

3. **Backcalculation Analysis:** The FWD deflection values were backcalculated to determine the stiffness of the pavement layers. Section 3.3.3 explains the backcalculation procedure.
4. **Structural Number (SN):** The structural number represents the effective structural strength of the existing pavement and base course. Four methods were used to calculate the SN based on FWD deflection values. Section 3.3.4 discusses these further.
5. **Impulse Stiffness Modulus (ISM):** The impulse stiffness moduli defines how much force is required to deflect the pavement by one millimeter and is a good way to identify test points with similar stiffness. Section 3.3.5 explains and discusses ISM values.

3.3.1 FWD center (maximum) deflection (D_0)

FWD maximum deflection indicates the structural capacity of the pavement structure. For pavement evaluation and design, this center deflection needs to be adjusted to a standard load of 9000 lbf (40 kN) for highways and corrected to a standard temperature of 20°C. In this study, the maximum deflections for each test point were first normalized to 9000 lbf (40 kN) and then corrected to a reference temperature of 20°C, as presented in equation (3) (Kim et al. 1995), using the measured mid-depth asphalt temperature:

$$D_{68} = D_T \times \left[10^{\propto(68-T)}\right], \tag{3}$$

where

D_{68} = the adjusted deflection (in.) to the reference temperature of 20°C (68°F),
D_T = the deflection (in.) measured at temperature T (°F),
α = $3.67 \times 10^{-4} \times t^{1.4635}$ for wheel paths and $3.65 \times 10^{-4} \times t^{1.4241}$ for lane centers,
t = the thickness of the asphalt layer (in.), and
T = the asphalt layer mid-depth temperature (°F) at the time of FWD testing.

Figure 21 illustrates an example of the normalized average deflection bowl to a 9000 lbf (40 kN) load with the associated standard deviation in the outer wheel path at drop 8 for each section. Noting that the plotted maximum deflection is displayed in mils (0.001 in.) and was corrected to 20°C (68°F). As the figure shows, the sections with polymer-modified asphalt

show relatively lower deflection values compared to the control section. This suggests that the polymer slightly improved the structural capacity of the sections regardless of the dosage rate. However, considering the standard deviation of the measured deflection for each section, all four sections exhibit similar behavior. Thus, comprehensive analysis of the FWD deflection bowl is needed to better assess the sections and to determine whether the polymer affects the overall performance of these sections, which is explained in subsequent sections.

Figure 21. Normalized deflection bowls for each test section. (Note: 1 mil = 25.4 um.)

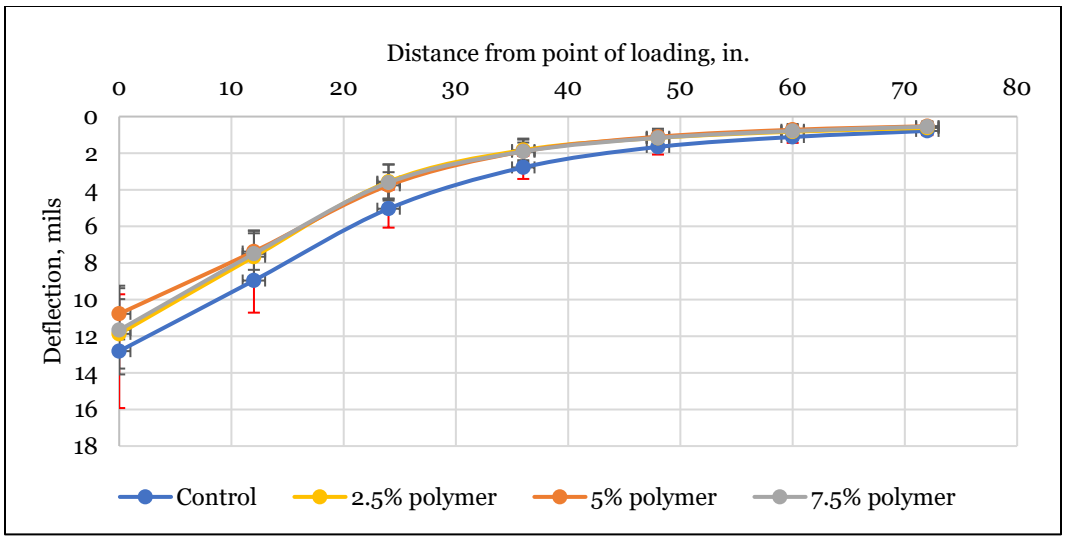

Figure 22 compares the corrected maximum deflection between the midlane and the outer wheel path. As expected, the deflection at the outer wheel path is higher than those measured at the midlane due to the impact of the traffic loading.

The pavement-condition threshold values were set for the maximum deflection based on the ESALs of less than 0.3 million (Noureldin et al. 2003). The sections were categorized as excellent, very good, good, and fair condition. They were determined by their average maximum deflection as follows:

- Excellent condition—Measurements < 12 mils
- Very good condition—Measurements 12–14 mils
- Good condition—Measurements 14–16 mils
- Fair condition—Measurements > 16 mils

An FWD deflection test was also conducted on the existing pavements (without an overlay) next to the overlay sections to understand the structural condition of the roadway before placing 2 in. (50 mm) of asphalt overlay. As Figure 22 shows, the old pavement before the overlay was in a fair condition. Then, placing the overlay layer enhanced the pavement to an excellent to very good condition. Appendix A shows the FWD deflection results for all sections.

Figure 22. Corrected maximum deflections in the test sections for the outer wheel path and midlane. (Note: 1 mil = 25.4 um.)

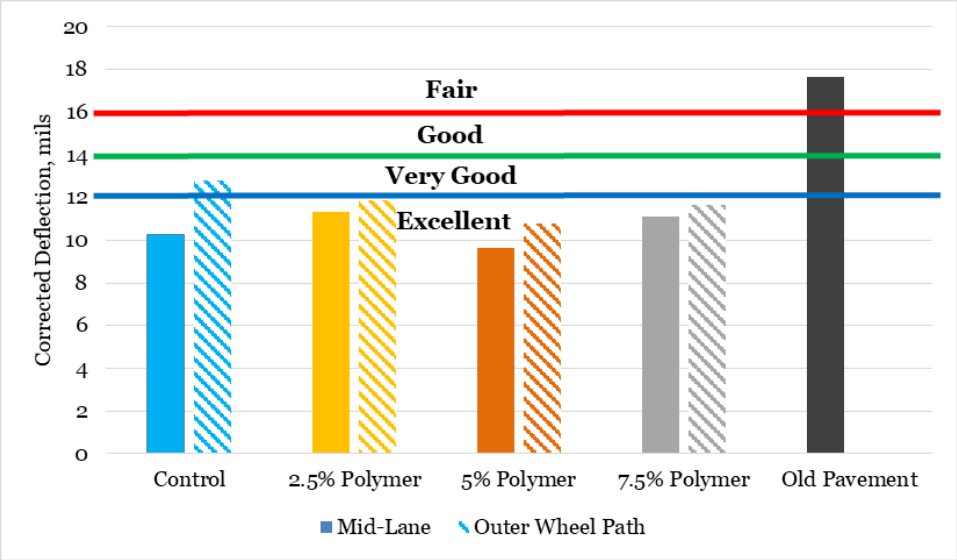

3.3.2 Deflection bowl parameters

The deflection bowl shape is another way to interpret the response of the pavement structure. Typically, the deflection bowls close to the loading plate represent the relative stiffness of the upper layers while the furthest deflection represents the stiffness of the subgrade layer (Tonkin et al. 1998). Typically, there are three slope parameters that represent the relative stiffness of pavement layers. The first parameter is the Surface Curvature Index (SCI), which is defined as the difference between the maximum deflection (D_0) and deflection at 12 in. (300 mm) from the plate load (D_{12}). This parameter tends to reflect the top 8 in (200 mm). of a flexible pavement structure. The second parameter is the Base Curvature Index (BCI), defined as deflection differences in the middle of the bowl about 12 to 36 in. (300 to 900 mm) from the center of the load. This parameter tends to reflect the relative stiffness of the middle layers (base and subbase) of a flexible pavement structure. The third parameter is the Lower Layer Index (LLI), defined as the differences between deflections at 36 and 48 in. (900

and 1200 mm). This parameter typically correlates very well with the subgrade layer.

This study set threshold values for each parameter based on suggestions by Rhode and Hartman (1996) (Table 9). The sections were categorized into Sound, Warning, and Severe conditions.

Table 9. Deflection bowl parameter thresholds.

Structural Condition Rating	Deflection Bowl Parameters Thresholds		
	SCI (µm)	BCI (µm)	LLI (µm)
Sound	<200	<100	<50
Warning	200–400	100–200	50–100
Severe	>400	>200	>100

Figure 23 presents the average deflection bowl parameters with the associated standard deviation for four sections. The SCI, BLI, and LLI parameters indicate that the upper, intermediate, and lower pavement layers are in a relatively sound condition. The BCI and LLI parameters for all four sections are relatively similar. However, SCI parameters of the four sections are slightly different. The section with 5% polymer has lower SCI measurements, which indicate a stronger, stiffer layer than other sections. This could indicate the contribution of polymer dosage in the structural capacity of the upper layer.

Figure 23. SCI, BCI, and LLI measurements for the four test sections.

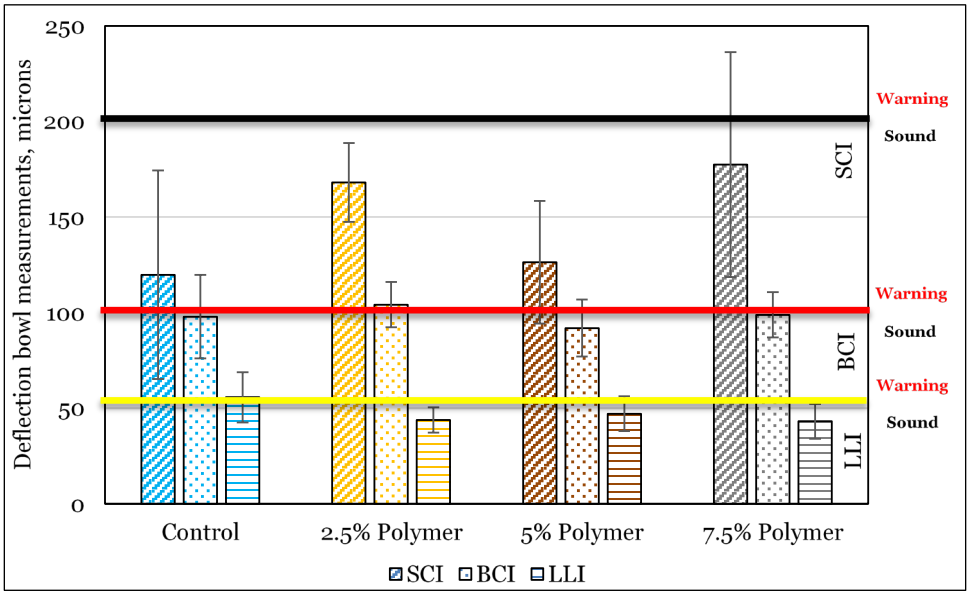

3.3.3 Backcalculation analysis

One of the most widely used technique for analyzing the measured FWD deflection bowls is backcalculation. The shape and the magnitude of FWD deflections can be used to predict the stiffness of pavement layers through backcalculation analysis. In this study, the backcalculation analysis was performed using Evaluation of Layer Moduli and Overlay Design (ELMOD) software. ELMOD performs layer elastic analysis to iteratively adjust the seed modulus for each layer to match the predicted and measured deflections within some tolerable error. The adequate range of tolerance error is considered 1% to 3% to estimate accurate modulus values for pavement layers.

To compare the modulus values of asphalt overlay layers among four sections, this study treated the asphalt layer as two individual layers in the backcalculation analysis; the top layer is a thin asphalt overlay, and the second layer is the old existing asphalt layer. However, a thin asphalt layer less than 75 mm is not recommended due to the associated high error (Pierce et al. 2017). Therefore, the current study made several attempts to minimize the associated errors to estimate a reasonable modulus value for each layer.

The backcalculation analysis used the followings input parameters:

1. Pavement-layer thickness: The thickness of asphalt overlay layers of four sections were determined from the field cores as shown in Figure 20. The old asphalt layer and base thickness were determined from the construction records.

2. Seed modulus values of the pavement layers:

    a. Asphalt Layer: The seed modulus value for the asphalt overlay layer was considered to be 500,000 psi (3447 MPa) at 20°C based on the dynamic modulus master curve conducted in the laboratory. The seed value for the old asphalt layer was assumed to be 150,000 psi (1034 MPa) at 20°C and treated as a fixed layer in the backcalculation analysis (Pierce et al. 2017).

    b. Base Layer: The seed modulus value for the FDR layer was assumed to be 60,000 psi (413 MPa) (AASHTO 2008).

c. Subgrade Layer: The resilient modulus of the subgrade at the time of the FWD measurements was determined from the measured moisture content. The soil samples from four depths (400, 475, 550, and 600 mm from the pavement surface) were collected and sent to the laboratory to measure the moisture contents in accordance with ASTM (2019a) D2216-19. The results of the moisture contents at the four depths were 30%. Then, the measured moisture content was converted to degree of saturation to be used in the Witczak's equation (Witczak et al. 2000), presented in equation (4), to determine the resilient modulus at the time of the FWD measurements. This resilient modulus value was considered to be the seed modulus value of the subgrade in the backcalculation analysis

$$\log \frac{\mathrm{Mr}}{\mathrm{Mr_{opt}}} = a + \frac{b-a}{1+\exp\left[ln\frac{-b}{a}+k_{\mathrm{m}}(S-S_{\mathrm{opt}})\right]}, \quad (4)$$

where

Mr = the resilient modulus at any degree of saturation,
$\mathrm{Mr/Mr_{opt}}$ = the resilient modulus ratio,
$\mathrm{Mr_{opt}}$ = the resilient modulus at a reference condition (determined from equation [2]),
a = the minimum of log $\mathrm{Mr/Mr_{opt}}$,
b = the maximum of log $\mathrm{Mr/Mr_{opt}}$,
k_{m} = the regression parameter, and
$S–S_{\mathrm{opt}}$ = the variation in degree of saturation expressed in decimals.

The backcalculation analysis used the measured FWD deflections in the outer wheel path at the last drop of the 9000 lbf (40 kN) load (drop 8). The FWD deflection measurements in the outer wheel path was selected to predict the modulus values because the pavement distress usually occurs in the wheel path. The backcalculation analysis assumed the depth to bedrock was very deep. The measured mid-depth temperature of the asphalt overlay layer was considered as the effective temperature to represent the asphalt layer temperature at the time of the FWD measurement (Chen et al. 2000). The backcalculated asphalt moduli were corrected to the standard temperature of 20°C using the asphalt temperature adjustment factor (ATAF) presented in equations (5) and (6) (Lukanen et al. 2000).

$$\mathrm{ATAF} = 10^{\mathrm{Slope}(T_{\mathrm{r}}-T_{\mathrm{m}})}, \quad (5)$$

$$E_{\text{corrected at reference temp}} = \text{ATAF} \times E_{\text{backcalculated at measured temp}}, \quad (6)$$

where

ATAF = the asphalt temperature adjustment factor,
Slope = Log (Mr)
T = −0.021 for the midlane and −0.0195 for the wheel path,
T_r = the reference mid-depth asphalt layer temperature,
T_m = the mid-depth asphalt layer temperature at the time of FWD testing (°C),
$E_{corrected}$ = corrected asphalt layer modulus to a reference temperature, and
$E_{backcalculated}$ = the backcalculated asphalt modulus at the temperature of the FWD testing.

Table 10 shows for the four sections the layer thickness, seed modulus values, and the corresponding corrected backcalculated modulus to a mid-depth asphalt temperature.

Table 10. Input values and modulus results for the backcalculation analysis. (asphalt overlay values are *bold*.)

Pavement Test Section	Pavement Layers	Thickness (mm)	Seed Values (MPa)	Backcalculated Modulus (MPa)		RMSE[a] (%)
				Mean	Std.	
Control	Asphalt overlay	53.3	3447	**12376**	**37**	1.9
	Old asphalt	96.5	1034	1034	0	
	Base	200	413	483	13	
	Subgrade		69	69	11	
2.5% polymer	Asphalt overlay	41.9	3447	**16099**	**14**	2.8
	Old asphalt	78.7	1034	1034	0	
	Base	200	413	414	14	
	Subgrade		69	83	10	
5% polymer	Asphalt overlay	50	3447	**13286**	**31**	3
	Old asphalt	99.0	1034	1034	0	
	Base	200	413	345	19	
	Subgrade		69	97	10	
7.5% polymer	Asphalt overlay	42.7	3447	**6812**	**52**	2.3
	Old asphalt	82.6	1034	1034	0	
	Base	200	413	483	17	
	Subgrade		69	93	11	

[a] Root-mean-square error

As the table shows, the backcalculated moduli of the asphalt overlay were on average 1.3 times higher in the section with 5% polymer and 1.07 times higher than in the section with 2.5% polymer than in the control section. This analysis suggests that the dosage of 2.5% and 5% polymer increased the stiffness of the asphalt overlay layer by 7% to 30%, respectively. It is worth noting that this increase in stiffness due to the polymer effects is based on one-time FWD measurements only. Further monitoring is needed to capture the impact of solid polymer on the short-term and long-term pavement performance.

The approach of the backcalculation analysis implemented in this study assumed a lower modulus value for the old asphalt layer to distinguish the performance of each polymer section compared to the control section. Also, the selection for the lower modulus value for the old asphalt layer was based on the distress survey discussed in section 2.1.4. However, in reality, the old asphalt layer becomes stiffer and more brittle due to the oxidation and aging and may develop cracks with repeated exposure to cold temperatures. This leads to a higher, stiffer modulus of the old asphalt layer due to aging, which could adversely affect the modulus of the asphalt overlay for the four sections if it was accounted for during the backcalculation analysis. That means the asphalt overlay modulus values shown in Table 10 could dramatically change, but the percent of increase in the asphalt overlay modulus for the polymer sections (i.e., 7%–30% increase depending on the dosage rate) may only slightly differ if the backcalculation analysis accounts for a stiffer old asphalt modulus.

3.3.4 Structural number determination

The SN is an index that represents the structural strength of the pavement. It accounts for the contribution of layer thickness, stiffness, and drainage capability of each layer in a pavement structure. This report presents four methods for determining the effective structural number (SN_{eff}) of the control and three polymer-modified asphalt sections, which is based on FWD deflections measured in the outer wheel path at the last drop of a 9000 lbf (40 kN) load. The following are the four approaches to determining the SN_{eff}.

3.3.4.1 AASHTO Non-Destructive Testing (NDT) approach

The AASHTO approach has been an important pavement design tool for several decades and has been widely used by pavement engineers due to

its simplicity. This approach can be an effective way of looking at differences in the structural capacity among four sections and of investigating the impact of polymer on the structural capacity of pavement sections. The SN_{eff} is calculated using the effective modulus of pavement layers above subgrade (E_p) in equation (7):

$$SN_{eff} = 0.0045 \times D \times \sqrt[3]{E_p}, \quad (7)$$

where

D = the total thickness of all layers above the subgrade (in.) and
E_p = the effective modulus of pavement layers above the subgrade (psi).

The effective modulus of pavement layers (E_p) is determined from equation (8) based on the total thickness (D), plate radius, and backcalculated subgrade (Mr) for a pavement cross section:

$$d_0 = 1.5Pa\left\{\frac{1}{Mr\sqrt{1+\left(\frac{D}{a}\sqrt[3]{\frac{E_p}{Mr}}\right)^2}} + \frac{\left[1-\frac{1}{\sqrt{1+\left(\frac{D}{a}\right)^2}}\right]}{E_p}\right\}, \quad (8)$$

where

d_o = the maximum deflection adjusted to a standard temperature of 68°F,
P = the load plate pressure (psi),
a = the load plate raduis (in.),
D = the total thickness of the pavement layes (in.),
Mr = the subgrade resilient modulus (psi), and
E_p = the effective modulus of all layers above the subgrade (psi).

To determine E_p, the resilient modulus of the subgrade (Mr) was first backcalculated based on deflections from the sensor located at 36 in.

(914 mm) away from the center of the loading plate as presented in equation (9). Table 11 shows the average values of Mr, E_p, and the corresponding SN_{eff} for each section.

$$\mathrm{Mr} = C\frac{0.24P}{d_r r}, \tag{9}$$

where

Mr = the backcalculated subgrade resilient modulus (psi),
C = a correction factor of 0.33,
P = the applied load (lb),
d_r = the deflection at a distance r from the center of the load (in.), and
r = the distance from center of load (in.).

Table 11. AASHTO structural number calculations.

Pavement section	Mr (psi)[a]	E_p (psi)	SN_{eff}
Control	12,649	252,987	3.7
2.5% polymer	16,053	160,532	3.1
5% polymer	18,819	188,198	3.4
7.5% polymer	17,913	125,391	2.8

[a] 1 psi = 0.00689476 MPa.

As Table 11 shows, the average SN_{eff} for all sections varied slightly due to differences in the effective modulus above the subgrade layer for each section. This analysis suggests that the AASHTO NDT method was slightly able to capture the impact of polymer on the structural capacity of each section.

3.3.4.2 Rohde (1994) approach

Another method of calculating the SN used Rohde's (1994) approach. Rohde (1994) developed his relationships using more information from the deflection bowl following the assumption of the peak deflection under the FWD plate. Rohde's approach proved that the pavement subgrade response can be determined from the deflection at an offset of 1.5 times the pavement thickness above the subgrade. To calculate the SN for each section, the structural index of the pavement (SIP) was first calculated as the difference between the maximum deflection and the deflection at 1.5 times the total thickness (equation [10]). Then, this study used equation (11) to

determine the SN. The normalized deflections to 9000 lbf (40 kN) and corrected maximum deflection to a reference temperature of 20°C were used in determining SIP, and therefore SN:

$$\mathrm{SIP} = D_0 - D_{1.5H_\mathrm{p}}, \tag{10}$$

$$\mathrm{SN} = K_1 \mathrm{SIP}^{K_2} D^{K_3}, \tag{11}$$

where

SIP = the pavement structural index (μm),
D_0 = the peak FWD deflection measured under a 40 kN load,
$D_{1.5H_\mathrm{p}}$ = the calculated FWD deflection at an offset of 1.5 times the pavement thickness, and
H_p = the total pavement thickness (mm).

The average SNs for all sections were relatively similar as shown in Table 12 due to the similarity in the deflection bowl as Figure 21 shows.

3.3.4.3 Watanatada et al. (1987) approach (i.e., World Bank approach)

This study computed the structural capacity by using the modified structural number (SNC) from the FWD maximum deflection value (D_0) for asphalt pavement (equation [12]). The maximum deflection was normalized to 9000 lb (40 kN) and corrected to a reference temperature of 20°C for reasonable comparison among four sections:

$$\mathrm{SNC} = 3.2 \times D_0^{-0.63}, \tag{12}$$

where

SNC = the modified structural number and
D_0 = the maximum deflection (mm).

Table 12 presents the SNC values for the four sections. The results indicate that the section with 5% polymer is slightly stiffer than the control and other polymer-modified sections. The SN results exhibit similar patterns compared to those obtained from the Rohde (1994) approach regardless of the magnitude of the SN.

3.3.4.4 Schnoor and Horak (2012) approach

Schnoor and Horak (2012) developed a relationship between the effective structural number and deflection bowl parameters that use the whole deflection bowl. Schnoor and Horak (2012) used two pavement sections in South Africa with detailed material properties, layer thickness, and FWD testing to correlate various deflection bowl parameters with SN as determined by Rohde 1994. Schnoor and Horak (2012) used a stepwise regression analysis to correlate the SN with various deflection bowl parameters. Equation (13) presents the correlation between the SN and the number of the deflection bowl parameters:

$$\mathrm{SN}_{\mathrm{eff}} = e^{5.12}\mathrm{BLI}^{0.31}A_{\mathrm{upp}}^{-0.78}, \tag{13}$$

where

$\mathrm{SN}_{\mathrm{eff}}$ = the effective SN at the time of FWD measurement, which is representing the structural layers above the subgrade layer;
e = the natural logarithm;
BLI = the slope parameter determined by the difference between D_0 and D_{300}; and
A_{upp} = the area parameter determined based on deflections measured at 0, 300, 600, and 900 mm, as presented in equation (14).

$$A_{\mathrm{upp}} = \frac{5D_0 - 2D_{300} - 2D_{600} - D_{900}}{2}. \tag{14}$$

The calculated $\mathrm{SN}_{\mathrm{eff}}$ values for each test section were relatively similar and followed the same pattern as Rohde (1994) and Watanatada et al. (1987) approaches (Table 12).

Table 12. Calculated structural numbers for the test sections.

Pavement Section	Structural Number (SN)			
	AASHTO	Rohde (1994)	Watanatada et al. (1987)	Schnoor and Horak (2012)
Control	3.7	3.0	6.7	6
2.5% polymer	3.1	2.8	6.5	5.6
5% polymer	3.4	3.1	7.1	6.1
7.5% polymer	2.8	2.7	6.5	5.6

Table 12 shows the difference in the average SNs for each method. For all sections, the Watanatada approach resulted in SNs slightly higher than the Schnoor and Horak approach, and AASHTO resulted in SNs slightly higher than those determined from the Rohde approach. Despite the magnitude of the SN, the Rohde, Watanatada, and Schnoor and Horak approaches seemed to follow the same patters for each test section.

This study analyzed which SN method would best reflect the actual structural strength for each test section. For each test section, the team correlated the deflection bowl parameters (i.e., SCI, BCI, and LLI) and the SN as determined by the four aforementioned methods. As an example, Figure 24 displays that the deflection bowl parameters for the control section correlated very well individually with SNs determined from three approaches: Watanatada, Schnoor and Horak, and Rohde. On the other hand, the deflection bowl parameters did not correlate with SNs determined from the AASHTO NDT method ($R^2 < 0.05$). The same conclusion held for each polymer-modified test section.

Figure 24. SCI, BCI, and LLI vs. structural number for the control section.

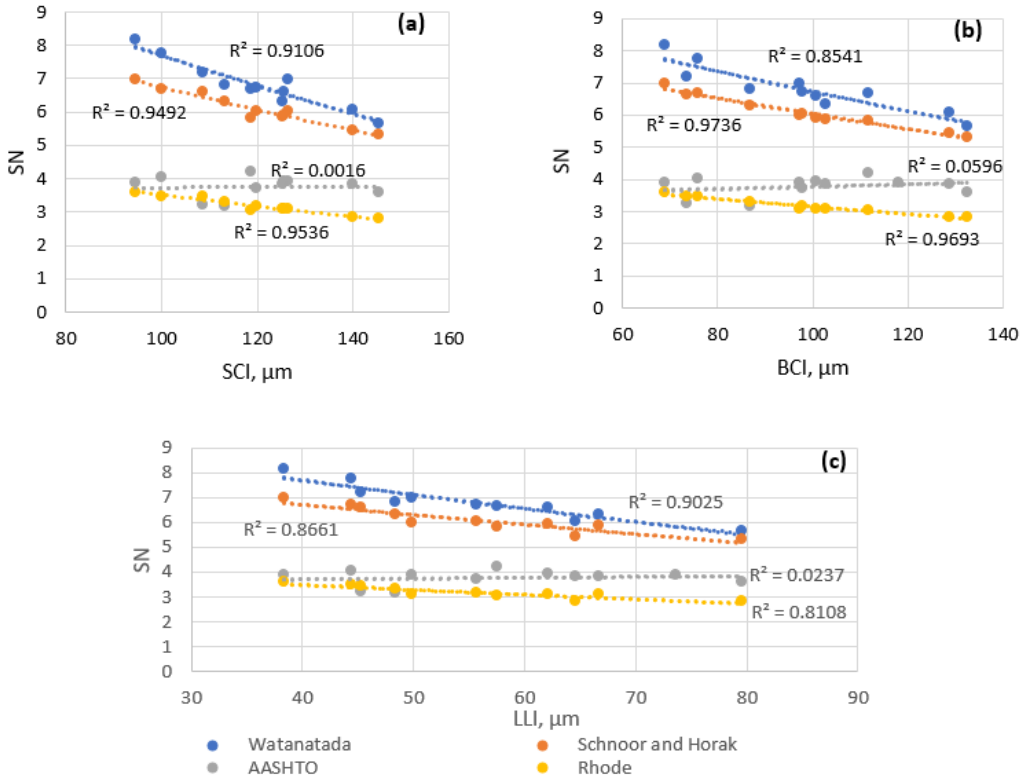

3.3.5 Impulse stiffness modulus (ISM)

The ISM defines how much force is required to deflect the pavement by one millimeter. ISM was calculated from the applied load and maximum deflection for each drop. It is used to identify test points with similar stiffness values. Figure 25 illustrates the calculated average ISM using the normalized maximum deflection to 9000 lbf (40 kN) and corrected to a reference temperature of 20°C at drop 8 in the outer wheel path. The higher the ISM, the stiffer the pavement section. Note that the section with 5% polymer is slightly stiffer than the control section. The calculated ISM values agree very well with the deflection bowl parameters and SN approaches in terms of the structural capacity and ranking for each test section.

Figure 25. Impulse stiffness modulus results for the test sections.

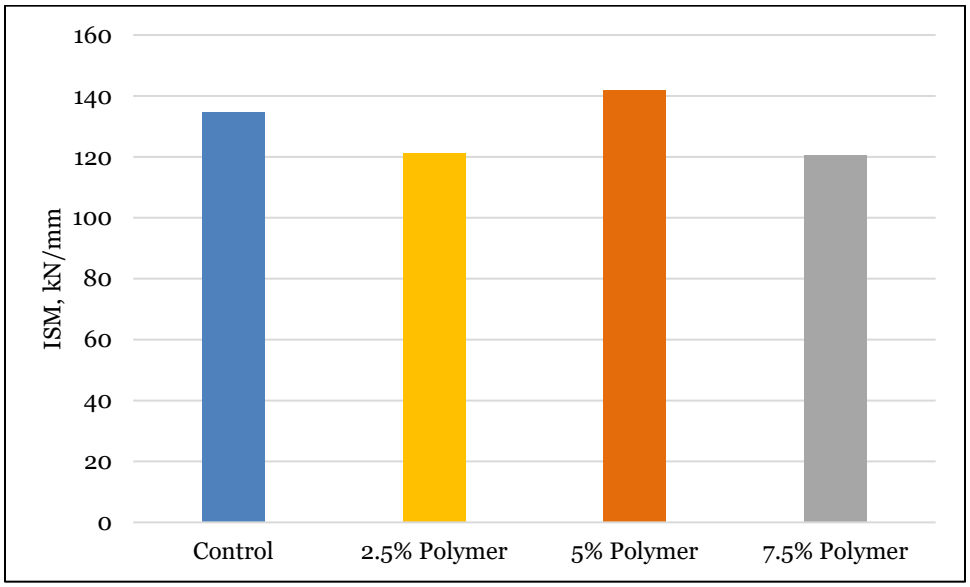

4 Cost Analysis

The objective of this chapter is to evaluate the life-cycle cost of four overlay mixtures (control, 2.5% polymer, 5% polymer, and 7.5% polymer) based on the field measurements of the FWD test. This chapter introduces the method used to calculate the fatigue life and discusses the life-cycle cost analysis of the four overlay mixtures.

4.1.1 Multilayer elastic analysis and fatigue results

This study used KENLAYER, multilayer elastic analysis computer software, to determine the pavement response to loading resulting from placing an overlay asphalt layer on top of old pavement. The horizontal tensile strain at the bottom of the asphalt overlay layer was computed given a load of a single-axle dual tire at 9000 lb (40 kN) with a contact radius of 4.89 in. (124.2 mm). The old asphalt and base layer thicknesses and backcalculated modulus of the control section, presented in Table 10 and Figure 26, were used in each KENLAYER analysis to calculate the horizontal strains. The Poisson's ratio of all the materials used in this analysis was obtained from the *Mechanistic-Empirical Pavement Design Guide* level 3 inputs: 0.35 for asphalt and base material and 0.40 for the subgrade layer (AASHTO 2008).

For each KENLAYER simulation (total of 12 simulations), the only two variables were the thickness and the modulus of the asphalt overlay layer as shown in Figure 26. For each overlay mixture type (four overlay mixtures), the KENLAYER analysis investigated three different overlay thicknesses (38 mm, 50 mm, and 76 mm) to identify the impact of overlay thickness on the life-cycle cost analysis. As presented in Figure 26, the KENLAYER analysis used the backcalculated modulus of each overlay mixture from the FWD test in Table 10 as the stiffness of the four overlay mixtures. The horizontal tensile strain at the bottom of the asphalt overlay layer was analyzed as it is related to bottom-up fatigue cracking in pavement. The maximum strain from different loading locations was used to calculate the number of cycles to fatigue failure.

Figure 26. Pavement cross section used in KENLAYER.

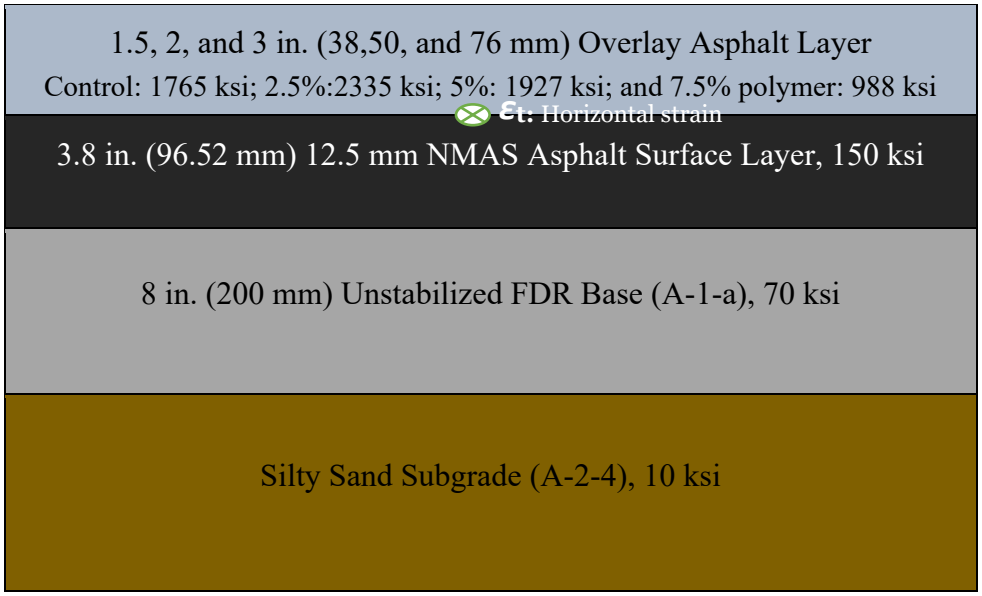

The maximum strains were then converted to the number of cycles to fatigue failure (N_f) using equation (15) developed for dense-graded asphalt mixture by the Minnesota Department of Transportation (Timm et al. 1999):

$$N_f = 2.83 \times 10^{-6} \left[\frac{10^6}{\varepsilon_t}\right]^{3.148}, \quad (15)$$

where

N_f = the number of load applications to fatigue cracking in 10% of the wheel path area and
ε_t = the horizontal tensile strain at the bottom of the asphalt layer (microstrain).

Table 13 shows the calculated horizontal strain values at the bottom of the overlay layer and the fatigue ratio of the four overlay mixtures at three different thicknesses. As observed in Table 13, the thickness of the overlay asphalt layer had an impact on the horizontal strain at the bottom of the overlay layer. The thinner overlay (50 mm) exhibited lower strain values while the thicker overlay (76 mm) exhibited higher strain values for all four overlay mixtures. The dosage of the solid polymer also impacted the horizontal strain values and fatigue performance. Additionally, the pavement section that was modified with a 7.5% polymer dosage exhibited

lower strain values at thin and intermediate overlay thickness and, therefore, higher fatigue life compared to the 2.5%, 5%, and control sections. The ratio of the number of cycles to fatigue failure of the polymer overlay mixtures to the number of cycles to fatigue failure of the control overlay mixture showed that the dosage of solid polymer had an impact on the fatigue life performance. The polymer-modified mixtures resulted in a fatigue ratio of up to 3.35 compared to the control mixture. This indicates that the polymer-modified mixture (7.5% polymer dosage) will have approximately up to a 230% increase in the fatigue life exhibited by the control section. The percent of increase in fatigue life was dependent on the solid-polymer dosage and overlay thickness as seen in Table 13.

Table 13. Mechanistic fatigue analysis results for the test sections.

Overlay thickness (mm)	Horizontal strain (microns)	N_f, cycles (million)	N_f Ratio (N_f/N_f Control)
Control Overlay Mixture			
38	106	9.21	1
50	133.4	4.47	1
76	140.30	3.81	1
2.5% Polymer Overlay Mixture			
38	114.10	7.30	0.792
50	132.80	4.53	1.013
76	131	4.73	1.242
5% Polymer Overlay Mixture			
38	109.10	8.41	0.913
50	133.70	4.43	1
76	137.6	4.05	1.063
7.5% Polymer Overlay Mixture			
38	72.19	30.85	3.350
50	120.20	6.20	1.387
76	150.80	3.04	0.798

4.1.2 Life-cycle cost analysis

The costs of the control and solid-polymer overlay layers were evaluated based on fatigue performance by using a single-lane pavement section 1 mile (1.64 km) long and 12 ft (3.66 m) wide. The mixture quantities required for paving 1.5 in. (38 mm), 2 in. (50 mm), and 3 in. (76 mm) were calculated as follows:

The 38 mm overlay

= 1600 m length × 3.66 m width × 0.0381 m thickness × 2338 kg/m^3 density

= 521,000 kg.

The 50 mm overlay

= 1600 m length × 3.66 m width × 0.0508 m thickness × 2338 kg/m^3 density

= 695,000 kg.

The 76 mm overlay

= 1600 m length × 3.66 m width × 0.0762 m thickness × 2338 kg/m^3 density

= 1,043,000 kg

The material cost for 1000 kg of modified mixture was calculated as follows:

- Control asphalt material cost per 1000 kg = $75.
- Solid-polymer cost per 1 kg = $3.50.
- Solid-polymer-modified-mixture material cost = control material cost + solid polymer cost.
- 2.5% polymer-modified-mixtures cost per 1000 kg = $75 + (1000 kg × 5.8% × 2.5% × $3.50) = $80.08.
- 5% polymer-modified-mixtures cost per 1000 kg = $75 + (1000 kg × 5.8% × 5.0% × $3.50) = $85.15.
- 7.5% polymer-modified-mixtures cost per 1000 kg = $75 + (1000 kg × 5.8% × 7.5% × 3.50) = $90.22

As the cost of overlay mixtures calculations show, there is an increase in the cost of solid-polymer mixtures of 6.67%, 13.5%, and 20.3% for 2.5% polymer, 5% polymer, and 7.5% polymer, respectively.

Table 14 shows the calculated total material cost to pave 1 mile (1.64 km) of a single lane of control and polymer-modified mixtures at three overlay thicknesses.

Table 14. Total material cost for 1.64 km sections.

Thickness (mm)	Cost ($/1000 kg)	Cost ($/1.64 km)
Control Overlay Mixture		
38	$75	39,075
50		52,125
76		78,225
2.5% Polymer Overlay Mixture		
38	$80.07	41,680
50		55,600
76		83,440
5% Polymer Overlay Mixture		
38	$85.15	44,363
50		59,179
76		88,811
7.5% Polymer Overlay Mixture		
38	$90.22	47,004
50		62,703
76		94,099

The next step is to compare the overlay mixture cost of these four overlay mixtures. To do so, the cost of overlay per 1000 cycles of fatigue life per 1 mile (1.64 km) of a single lane was calculated (Table 15).

As Table 15 shows, the cost of 2.5% and 5% polymer-modified overlay per 1000 cycles of fatigue life per 1.64 km was higher than those in the control overlay mixture. However, a 7.5% polymer-modified overlay mixture showed an opposite trend at thin (38 mm) and intermediate (50 mm) thicknesses. This is due to the high number of cycles to failure seen in these sections. The lowest cost of overlay per 1000 cycles of fatigue life per 1.64 km was for the thin overlay modified with 7.5% polymer, which was $1.52.

The last step was to scrutinize the cost-effectiveness of each mixture by investigating the differences between the paid cost and gained benefits. This can be computed by dividing the expected fatigue performance of each mixture by its mixture unit cost. Table 15 shows the cost-effectiveness of all four overlay mixtures. As shown, the thickness of the overlay had an

impact on the cost-effectiveness of the overlay mixtures. The thin overlay (38 mm) was more cost-effective than the thick overlay (76 mm) for the control and three polymer overlay mixtures. For thin and intermediate overlay (38 mm and 50 mm), 7.5% polymer was the most cost-effective. For thick overlay (76 mm), the 2.5% polymer overlay mixture was more cost-effective than any other overlay mixtures.

Table 15. Cost-effectiveness measures of various material-thickness combinations.

Thickness (mm)	Cost ($/ton)	Cost of Overlay/ 1000 Cycles ($)	Cost ($/ 1.64 km)	Cost-Effectiveness (₦/cost)	Cost-Effectiveness Ratio
Control Overlay Mixture					
38	$75	4.24	39,075	235.63	1
50		11.67	52,125	85.65	1
76		20.53	78,225	48.70	1
2.5% Polymer Overlay Mixture					
38	$80	5.71	41,680	175.20	0.74
50		12.27	55,600	81.45	0.95
76		17.65	83,440	56.66	1.16
5% Polymer Overlay Mixture					
38	$85.15	5.28	44,363.15	189.54	0.81
50		13.35	59,179.25	74.91	0.87
76		21.93	88,811.45	45.60	0.94
7.5% Polymer Overlay Mixture					
38	$90.22	1.52	47,004.62	656.39	2.80
50		10.11	62,702.9	98.85	1.16
76		31	94,099.46	32.25	0.66

Table 15 also shows that the polymer dosage had an impact on the cost-effectiveness of the overlay mixtures. The pavement section that was modified with a dosage of 7.5% polymer was on average more cost-effective than all other overlay mixtures. The cost-effectiveness ratio of 7.5% polymer overlay mixture to the control overlay mixture was up to 2.80, which was higher than the other polymer overlay mixtures. This indicates that a 7.5% polymer overlay mixture is the most cost-effective overlay mixture of all the presented overlay mixtures. The results also suggested that the 5% polymer overlay mixture was not as cost-effective when compared with the control mixture.

Note that the presented life-cycle cost analysis approach is based on fatigue life only without considering the rutting and transverse cracking

lives, which will significantly impact the performance of pavements. Future work will include a comprehensive life-cycle cost analysis based on the fatigue, rutting, and transverse cracking from the laboratory and field testing to better assess the solid-polymer overlay mixtures.

5 Summary and Conclusions

This study constructed four test sections on Corbin Road located in Newport, New Hampshire: control (with no polymer), 2.5% polymer, 5% polymer, and 7.5% polymer. The asphalt mixture for the control test section was plant produced using a Superpave mix design with a PG 64-22 binder. The asphalt mixtures for the three other sections were modified using solid polymer, which was added during the plant production. The density for each test section was measured during the construction with nuclear gauge and three cores for each test section were extracted for density and thickness verification.

Field investigation, including the FWD testing, was conducted at each test section shortly after site construction to evaluate the structural capacity and to identify the structural benefits of adding solid polymer to the pavement sections. A comprehensive analysis evaluated the measured FWD deflection data for each test section to fulfill the goal of this study. The maximum pavement deflection, deflection bowl parameters, backcalculation analysis, SN, and impulse stiffness moduli approaches were conducted to assess each test section. ELMOD software was used to backcalculate the FWD deflections to estimate the stiffness of pavement layers for each test section. Four SN approaches were applied for each test section: AASHTO (1993), Rohde (1994), Watanatada et al. (1987), and Schnoor and Horak (2012) to investigate which approach captures the effect of solid polymer on the structural capacity of pavement sections. The calculated SN for each test section was determined from the measured FWD deflection bowls.

The study's cost-analysis approach used the field measurements of the FWD test to identify which overlay mixture is the most cost-effective. Multilayer elastic analysis was performed to compute the horizontal strain at the bottom of the overlay layer. The horizontal strains were then converted to the number of cycles to fatigue failure using a well-established transfer function. The fatigue performance and the cost-effectiveness of the control mixture, 2.5% polymer mixture, 5% polymer mixture, and 7.5% polymer mixture were calculated and compared.

The study concluded the following:

- The maximum deflection approach showed that the addition of polymer slightly improved the structural capacity of the pavement structure.

- The deflection bowl parameters (SCI, BCI, and LLI) approach demonstrated that the section with 5% polymer had a stiffer upper layer than the other sections.

- The backcalculation analysis revealed that the dosage of 2.5% and 5% polymer increased the stiffness of the asphalt overlay layer by 7% and 30% respectively compared to the conventional control section. Note that this increase in stiffness is based on one-time FWD measurements and the backcalculation approach utilized in this study by assuming a lower stiffness value for old asphalt layer. In other respects, the percent of increase in stiffness of the asphalt overlay layer for polymer sections will be slightly changed or not changed at all. Further investigations are needed to capture the short-term and long-term impact of solid polymer on the performance of an asphalt overlay layer.

- The structural number approaches exhibited that the SN values for each section varied depending on the approach used to calculate the SN. The Watanatada and the Schnoor and Horak approaches generated the highest and most similar SN values compared to the Rohde and AASHTO NDT approaches. Despite the differences in the calculated SN from each approach, the SN from the Rohde, Watanatada, and Schnoor and Horak approaches showed the benefits of adding polymer to the asphalt layer and followed the same pattern of ranking the structural capacity for each test section. In other words, the modified section with 5% polymer had the highest structural capacity out of all the sections. Conversely, the AASHTO NDT method showed no significant structural benefits of adding polymer.

- The impulse stiffness moduli approach revealed that the section with 5% polymer was slightly stiffer than the control section and other polymer-modified sections.

- The overlay mixture that was modified with a 7.5% solid-polymer dosage showed up to a 230% increase in fatigue life compared to the control mixture.

- The fatigue-life ratios were more sensitive to the overlay thickness than polymer dosage.

- Thinner overlay thickness resulted in a lower cost per 1000 cycles of fatigue life per 1.64 km for all four overlay mixtures. The cost per 1000 cycles of fatigue life increased as the overlay got thicker. The lowest cost of overlay per 1000 cycles of fatigue life was for 7.5% polymer.

- The thickness and polymer dosage impacted the cost-effectiveness of the overlay mixtures when only the initial construction was considered. The mixture modified with a 7.5% polymer dosage was the most cost-effective overlay mixture among all of the overlay mixtures, which was 2.80 times less costly than the control mixture. For a thicker overlay layer, 2.5% polymer dosage was more cost-effective than any other overlay mixtures, which was 1.2 times less costly than the control mixture. A 5% polymer overlay mixture was not a cost-effective mixture compared to the control mixture. Note that this analysis was based on the fatigue life that was predicted from the FWD test. Further investigation including the rutting and transverse cracking performance, which will impact the cost analysis, is still needed. Future work will showcase a more comprehensive life-cycle cost analysis based on laboratory and field testing.

The presented approaches agreed well with each other in terms of the ranking of structural capacity and stiffness for each test section. From the results obtained from the aforementioned investigations, the addition of solid polymer created structural benefits for the asphalt layer and the overall pavement structure. The solid polymer also eliminated the associated cost, poor workability, and storage stability concerns of liquid polymer binders. Therefore, it has the potential to be used in remote areas without any storage stability concerns during production and construction. However, further laboratory and field investigations considering the fatigue, rutting, and transverse cracking performance are still needed to showcase the potential to improve the structural capacity of pavement, to increase the pavement service life, and to show cost savings. Also, the long-term performance of these test sections still needs to be tracked over

time to examine the impact of polymer under different environmental conditions. Ultimately, the use of solid-polymer additives in asphalt mixtures shows promise for the Army and other military agencies who want to enhance flexible pavement performance in remote regions and expedient construction where traditional forms of modification may not be practical.

References

AASHTO (American Association of State Highway and Transportation Officials). 2008. *Mechanistic-Empirical Pavement Design Guide: A Manual of Practice Interim Edition*, Washington, D.C.: American Association of State Highway and Transportation Officials. https://www.google.com/books/edition/Mechanistic_empirical_Pavement_Design_Gu/3_h7Hbn5AZgC?hl=en&gbpv=1&printsec=frontcover.

———. 2017a. *Standard Specification for Performance-Graded Asphalt Binder*. Designation M320-17. Washington, DC: American Association of State Highway and Transportation Officials.

———. 2017b. *Standard Specification for Superpave Volumetric Mix Design*. Designation M323-17. Washington, DC: American Association of State Highway and Transportation Officials.

ASTM International. 2012. *Standard Test Methods for Laboratory Compaction Characteristics of Soil Using Standard Effort (12 400 ft-lbf/ft³ (600 kN-m/m³))*. ASTM D698-12e2. West Conshohocken, PA: ASTM International. https://doi.org/10.1520/D0698-12E02.

———. 2015a. *Standard Test Method for Relative Density (Specific Gravity) and Absorption of Coarse Aggregate*. ASTM C127-15. West Conshohocken, PA: ASTM International. https://doi.org/10.1520/C0127-15.

———. 2015b. *Standard Test Method for Relative Density (Specific Gravity) and Absorption of Fine Aggregate*. ASTM C128-15. West Conshohocken, PA: ASTM International. https://doi.org/10.1520/C0128-15.

———. 2017a. *Standard Test Methods for Quantitative Extraction of Asphalt Binder from Asphalt Mixtures*. ASTM D2172M-17e1. West Conshohocken, PA: ASTM International. https://doi.org/10.1520/D2172_D2172M-17E01.

———. 2017b. *Standard Test Methods for Liquid Limit, Plastic Limit, and Plasticity Index of Soils*. ASTM D4318-17e1. West Conshohocken, PA: ASTM International. https://doi.org/10.1520/D4318-17E01.

———. 2017c. *Standard Test Methods for Particle-Size Distribution (Gradation) of Soils Using Sieve Analysis*. ASTM D6913-17. West Conshohocken, PA: ASTM International. https://doi.org/10.1520/D6913_D6913M-17.

———. 2019a. *Standard Test Method for Theoretical Maximum Specific Gravity and Density of Asphalt Mixtures*. ASTM D2041-19. West Conshohocken, PA: ASTM International. https://doi.org/ 10.1520/D2041_D2041M-19.

———. 2019b. *Standard Test Methods for Laboratory Determination of Water (Moisture) Content of Soil and Rock by Mass*. ASTM D2216-19. West Conshohocken, PA: ASTM International. https://doi.org/10.1520/D2216-19.

———. 2019c. *Standard Test Method for Bulk Specific Gravity and Density of Non-Absorptive Compacted Asphalt Mixtures*. ASTM D2726-19. West Conshohocken, PA: ASTM International. https://doi.org/ 10.1520/D2726_D2726M-19.

Azam, A. M., S. M. El-Badawy, and R. M. Alabasse. 2019. "Evaluation of Asphalt Mixtures Modified with Polymer and Wax." *Innovative Infrastructure Solutions 4* (1): 43.

Bates, R., and R. Worch. 1987. *Styrene-Butadiene Rubber Latex Modified Asphalt*. Engineering Brief No. 39. Washington, DC: Federal Aviation Administration.

Brûlé, B. 1996. "Polymer-Modified Asphalt Cements Used in the Road Construction Industry: Basic Principles." *Transportation Research Record* 1535 (1): 48–53. Washington, DC: Transportation Research Board, National Research Council.

Chen, D. H., J. Bilyeu, H. H. Lin, and M. Murphy. 2000. "Temperature Correction on Falling Weight Deflectometer Measurements". *Transportation Research Record* 1716:30–39. Washington, DC: Transportation Research Board, National Research Council.

Collins, J. H. 1995. Method for obtaining Polymer/Bitumen Blends with Improved Stability and Polymer Efficiency. U.S. Patent Application No. US08/160,005, filed 30 November 1993. https://patents.google.com/patent/USH1484H/en.

Federal Highway Administration. 2016a. Long-Term Pavement Performance Bind Online Tool. Washington, DC: Federal Highway Administration. https://infopave.fhwa.dot.gov/Tools/LTPPBindOnline.

———. 2016b. *LTPP Climate Tool User Guide*. Report No. HRT-17-012. Washington, DC: Federal Highway Administration.

Isacsson, U., and H. Zeng. 1998. Low-Temperature Cracking of Polymer-Modified Asphalt. *Materials and Structures* 31 (1): 58–63.

Iterchimica. 2008. *Iterchimica SUPERPLAST: Additive for High Modulus Pavements*. Suisio, Italy: Iterchimica. https://www.academia.edu/11162770/SUPERPLAST_-_ACCREDITATION_OF_NEW_MATERIALS_AND_TECHNIQUES_-_REV3_final?auto=download.

Kim, Y. R., B. O. Hibbs, and Y. C. Lee. 1995. "Temperature Correction of Deflections and Backcalculated Asphalt Concrete Moduli." *Transportation Research Record 1473*, 55–62.Washington, DC: Transportation Research Board, National Research Council.

King, G., H. King, R. D. Pavlovich, A. L. Epps, and P. Kandhal. 1999. "Additives in asphalt." *Journal of the Association of Asphalt Paving Technologists* 68:32–69.

Lukanen, E. O., R. Stubstad, and R. Briggs. 2000. *Temperature Predictions and Adjustment Factors for Asphalt Pavement*. FHWA-RD-98-085. McLean, VA: Federal Highway Administration. https://rosap.ntl.bts.gov/view/dot/15368.

Miller, J. S., and W. Y. Bellinger. 2014. *Distress Identification Manual for the Long-Term Pavement Performance Program*. FHWA-HRT-13-092. McLean, VA: Federal Highway Administration, Office of Infrastructure Research and Development. https://rosap.ntl.bts.gov/view/dot/40882.

Newcomb, D. 2003. "Limit the Strain at the Bottom of an Asphalt Pavement, and What Do You Get?: A Perpetual Pavement." *HMAT: Hot Mix Asphalt Technology 8* (6): 30–32.

Newman, J. K. 2003. "Flexural Beam Fatigue Properties of Airfield Asphalt Mixtures Containing Styrene-Butadiene Based Polymer Modifiers." In Proceedings of the *Sixth International RILEM Symposium on Performance Testing and Evaluation of Bituminous Materials*, 357–363. Bagneux, France: RILEM Publications SARL.

Noureldin, A. S., K. Zhu, S. Li, and D. Harris. 2003. "Network Pavement Evaluation Using Falling Weight Deflectometer and Ground Penetrating Radar." *Transportation Research Record 1860*, 90–99.Washington, DC: Transportation Research Board, National Research Council

Pierce, L. M., J. E. Bruinsma, K. D. Smith, M. J. Wade, K. Chatti, and J. Vandenbossche. 2017. *Using Falling Weight Deflectometer Data with Mechanistic-Empirical Design and Analysis, Volume III: Guidelines for Deflection Testing, Analysis, and Interpretation*. FHWA-HRT-16-011. McLean, VA: U.S. Federal Highway Administration.

Rohde, G. T. 1994. "Determining Pavement Structural Number from FWD Testing." *Transportation Research Record* 1448:61–68. Washington, DC: Transportation Research Board, National Research Council Academies.

Schmalzer, P. N. 2006. *Long-Term Pavement Performance Program Manual for Falling Weight Deflectometer Measurements*. FHWA-HRT-06-132. McLean, VA: U.S. Federal Highway Administration, Office of Infrastructure Research and Development. https://www.fhwa.dot.gov/publications/research/infrastructure/pavements/ltpp/06132/.

Schnoor, H., and E. A. Horak. 2012. "Possible Method of Determining Structural Number for Flexible Pavements with the Falling Weight Deflectometer." In *Proceedings of the Southern African Transportation Conference*, Pretoria, South Africa, 9–12 July 2012. http://hdl.handle.net/2263/20033.

Timm, D., D. Newcomb, and B. Birgisson. 1999. *Mechanistic-Empirical Flexible Pavement Thickness Design: The Minnesota Method*. MN/RC-P99-10. St. Paul, MN: Minnesota Department of Transportation. http://dotapp7.dot.state.mn.us/research/pdf/P199910.pdf.

Tonkin and Taylor. 1998. *Pavement Deflection Measurement and Interpretation for the Design of Rehabilitation Treatments*. Transfund New Zealand Research Report No. 117. Wellington, New Zealand: Transfund New Zealand. https://www.nzta.govt.nz/assets/resources/research/reports/117/117-Pavement-deflection-measurement-and-interpretation-for-the-design-of-rehabilitation-treatments.pdf.

Watanatada, T., C. G. Harral, W. D. Paterson, A. M. Dhareshwar, A. Bhandari, and K. Tsunokawa. 1987. *The Highway Design and Maintenance Standards Model. Volume 1, Description of the HDM-III Model. Volume 2, User's Manual for the HDM-III Model*. World Bank Highway Design and Maintenance Standards Series. Washington, DC: World Bank. https://trid.trb.org/view/451315.

Wegan, V. 2001. *Effect of Design Parameters on Polymer Modified Bituminous Mixtures*. Copenhagen, Denmark: Danish Road Directorate. https://trid.trb.org/view/731828.

Witczak, M. W., W. N. Houston, and D. Andrei. 2000. *Resilient Modulus as Function of Soil Moisture—A Study of the Expected Changes in Resilient Modulus of the Unbound Layers with Changes in Moisture for 10 LTPP Sites*. Development of the 2002 Guide DD-3.35 for the Development of New and Rehabilitated Pavement Structures. NCHRP 1-37 A. Inter Team Technical Report (Seasonal 2).

Appendix A: Supplementary Figures

Figure A-1. The corrected maximum deflections in the control test section for the outer wheel path.

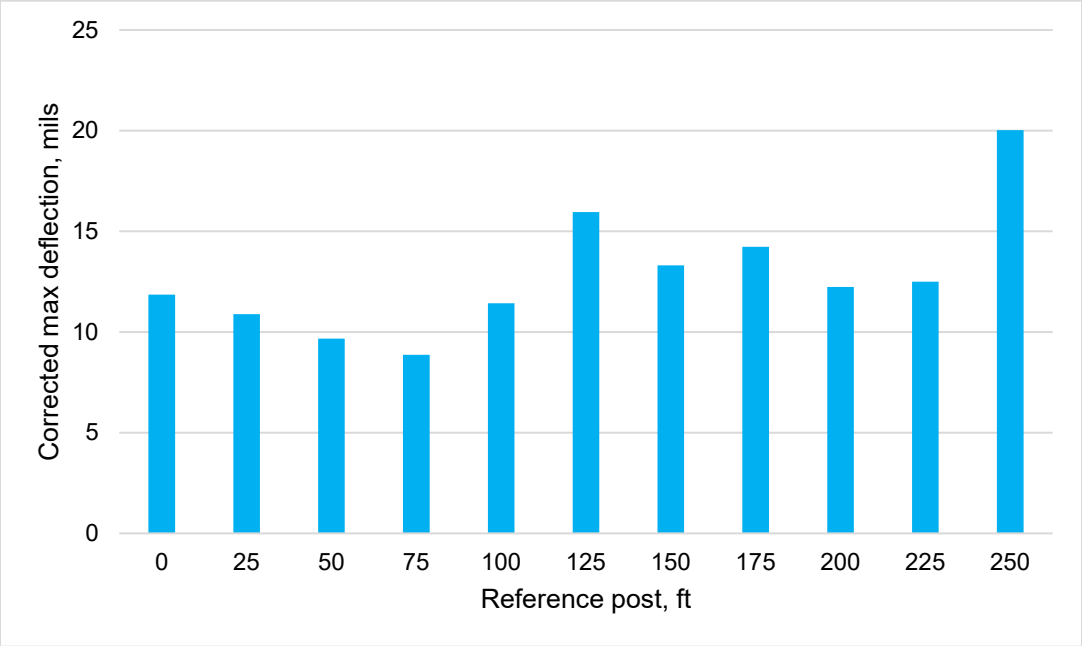

Figure A-2. The corrected maximum deflections in the 2.5% polymer test section for the outer wheel path.

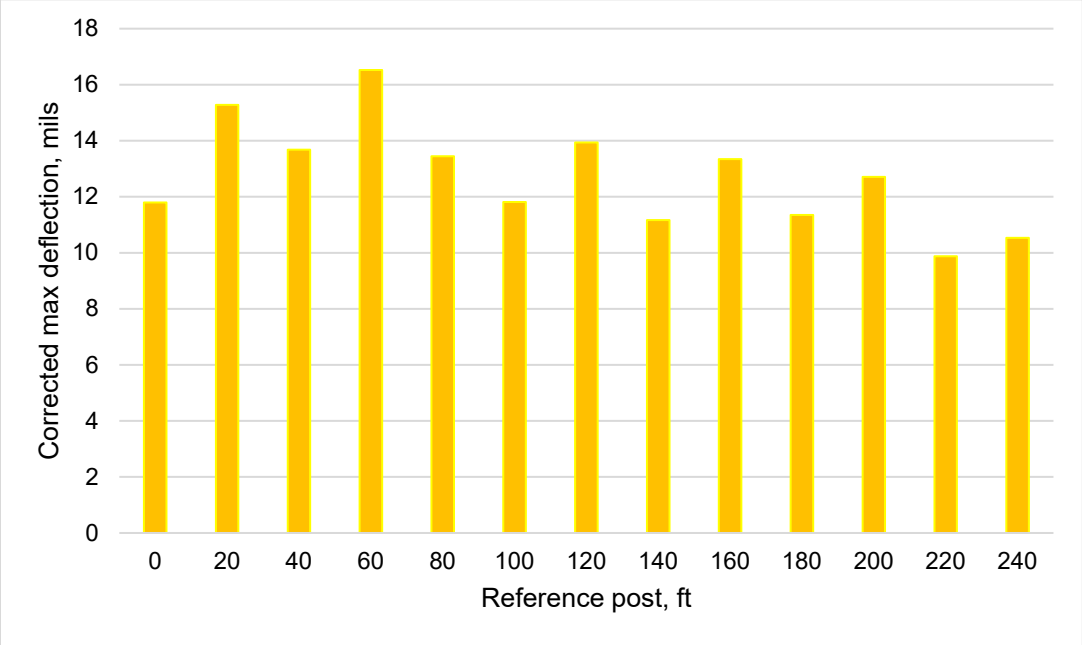

Figure A-3. The corrected maximum deflections in the 5% polymer test section for the outer wheel path.

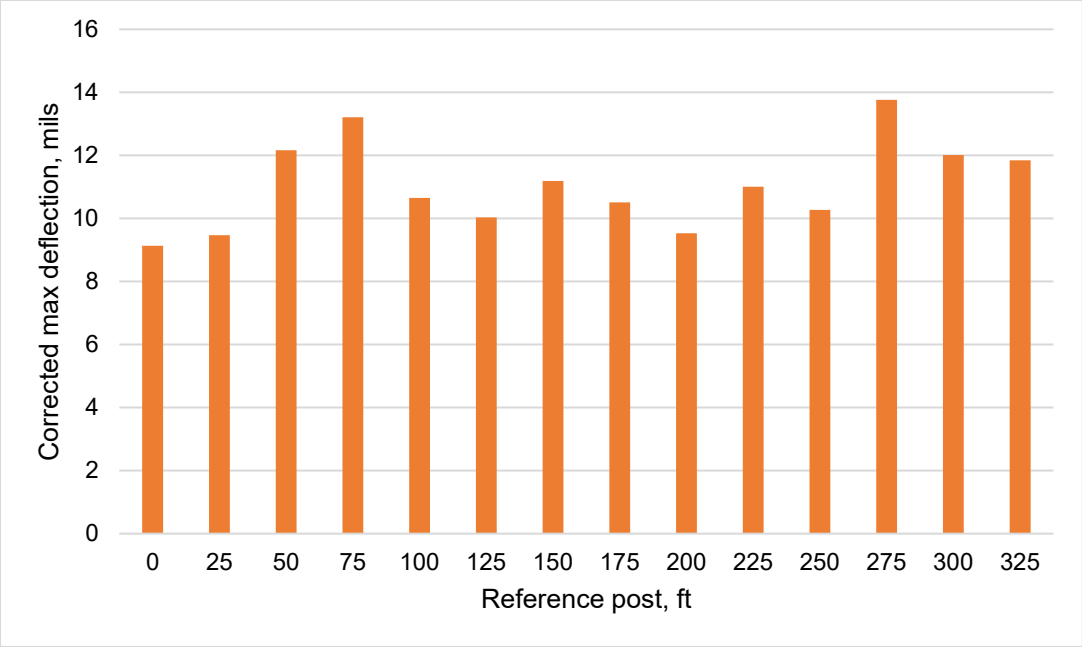

Figure A-4. The corrected maximum deflections in the 7.5% polymer test section for the outer wheel path.

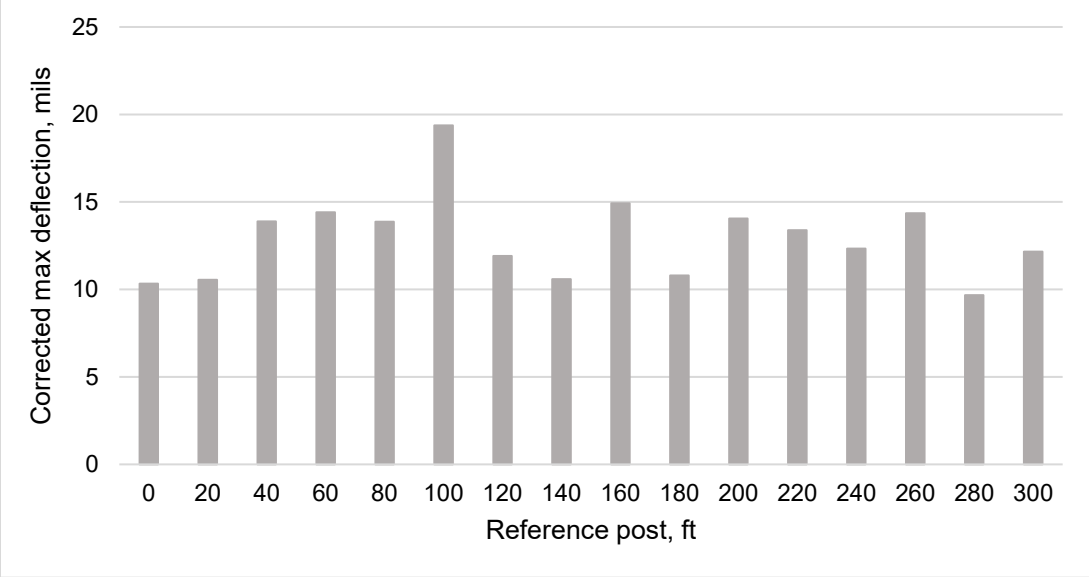

REPORT DOCUMENTATION PAGE

Form Approved
OMB No. 0704-0188

1. REPORT DATE (DD-MM-YYYY)	2. REPORT TYPE	3. DATES COVERED (From - To)
September 2020	Technical Report / Final	FY18–FY19

4. TITLE AND SUBTITLE

Evaluation of Solid-Polymer-Modified Asphalt Mixtures:
Phase 1: Construction and Performance Testing of Field Pavement Sections

5a. CONTRACT NUMBER

5b. GRANT NUMBER

5c. PROGRAM ELEMENT
62784

6. AUTHOR(S)
Christopher J. DeCarlo, Mohamed H. Elshaer, Allan Wheeler, and Jared I. Oren

5d. PROJECT NUMBER
T26

5e. TASK NUMBER

5f. WORK UNIT NUMBER

7. PERFORMING ORGANIZATION NAME(S) AND ADDRESS(ES)
U.S. Army Engineer Research and Development Center (ERDC)
Cold Regions Research and Engineering Laboratory (CRREL)
72 Lyme Road
Hanover, NH 03755-1290

8. PERFORMING ORGANIZATION REPORT NUMBER
ERDC/CRREL TR-20-11

9. SPONSORING / MONITORING AGENCY NAME(S) AND ADDRESS(ES)
Headquarters, U.S. Army Corps of Engineers
Washington, DC 20314-1000

10. SPONSOR/MONITOR'S ACRONYM(S)
USACE

11. SPONSOR/MONITOR'S REPORT NUMBER(S)

12. DISTRIBUTION / AVAILABILITY STATEMENT
Approved for public release; distribution unlimited.

13. SUPPLEMENTARY NOTES

14. ABSTRACT

The durability of flexible pavements in cold regions is a challenge due to the impact of environmental conditions and seasonal variations. Other studies have investigated several modifiers as potential solutions to address cold climate durability of asphalt mixtures. Among these modifiers, polymer modification has shown promise.

This study investigated the addition of solid polymer to asphalt mixtures to improve the performance and structural capacity of the material. Four test sections were constructed with different solid-polymer dosage rates: unmodified control, 2.5% polymer, 5% polymer, and 7.5% polymer by weight of binder. Falling weight deflectometer (FWD) testing was conducted at each test section to evaluate the structural capacity and to identify the performance benefits of the solid-polymer-modified mixtures. This study conducted a comprehensive analysis, including maximum pavement deflection, deflection bowl parameters, backcalculation analysis, structural number, and impulse stiffness modulus.

The field investigation results revealed structural benefits in test sections with the solid-polymer-modified mixture (7%–30% increase in stiffness, depending on the dosage rate). Results suggest that solid-polymer modification could be useful in improving the stiffness of asphalt pavements without compromising durability. Therefore, further investigations should evaluate the durability of the solid-polymer-modified asphalt pavements under different environmental conditions.

15. SUBJECT TERMS
Pavements, Flexible--Cold regions, Pavements, Flexible--Service life, Polymer asphalt—Evaluation, Polymer asphalt--Testing

16. SECURITY CLASSIFICATION OF:			17. LIMITATION OF ABSTRACT	18. NUMBER OF PAGES	19a. NAME OF RESPONSIBLE PERSON
a. REPORT	b. ABSTRACT	c. THIS PAGE			19b. TELEPHONE NUMBER (include area code)
Unclassified	Unclassified	Unclassified	SAR	73	